



National Library
of Canada

Bibliothèque nationale
du Canada

Canadian Theses Service

Services des thèses canadiennes

Ottawa, Canada
K1A 0N4

CANADIAN THESES

THÈSES CANADIENNES

NOTICE

The quality of this microfiche is heavily dependent upon the quality of the original thesis submitted for microfilming. Every effort has been made to ensure the highest quality of reproduction possible.

If pages are missing, contact the university which granted the degree.

Some pages may have indistinct print especially if the original pages were typed with a poor typewriter ribbon or if the university sent us an inferior photocopy.

Previously copyrighted materials (journal articles, published tests, etc.) are not filmed.

Reproduction in full or in part of this film is governed by the Canadian Copyright Act, R.S.C. 1970, c. C-30.

AVIS

La qualité de cette microfiche dépend grandement de la qualité de la thèse soumise au microfilmage. Nous avons tout fait pour assurer une qualité supérieure de reproduction.

S'il manque des pages, veuillez communiquer avec l'université qui a conféré le grade.

La qualité d'impression de certaines pages peut laisser à désirer, surtout si les pages originales ont été dactylographiées à l'aide d'un ruban usé ou si l'université nous a fait parvenir une photocopie de qualité inférieure.

Les documents qui font déjà l'objet d'un droit d'auteur (articles de revue, examens publiés, etc.) ne sont pas microfilmés.

La reproduction, même partielle, de ce microfilm est soumise à la Loi canadienne sur le droit d'auteur, SRC 1970, c. C-30.

**THIS DISSERTATION
HAS BEEN MICROFILMED
EXACTLY AS RECEIVED**

**LA THÈSE A ÉTÉ
MICROFILMÉE TELLE QUE
NOUS L'AVONS REÇUE**

THE UNIVERSITY OF ALBERTA

FLUID INCLUSION AND STABLE ISOTOPE STUDIES OF THE GOLD
DEPOSITS IN OKANAGAN VALLEY, BRITISH COLUMBIA

by

XIAOMAO ZHANG

A THESIS

SUBMITTED TO THE FACULTY OF GRADUATE STUDIES AND RESEARCH
IN PARTIAL FULFILMENT OF THE REQUIREMENTS FOR THE DEGREE
OF MASTER OF SCIENCE

DEPARTMENT OF GEOLOGY

EDMONTON, ALBERTA

FALL, 1986

Permission has been granted to the National Library of Canada to microfilm this thesis and to lend or sell copies of the film.

The author (copyright owner) has reserved other publication rights, and neither the thesis nor extensive extracts from it may be printed or otherwise reproduced without his/her written permission.

L'autorisation a été accordée à la Bibliothèque nationale du Canada de microfilmer cette thèse et de prêter ou de vendre des exemplaires du film.

L'auteur (titulaire du droit d'auteur) se réserve les autres droits de publication; ni la thèse ni de longs extraits de celle-ci ne doivent être imprimés ou autrement reproduits sans son autorisation écrite.

ISBN 0-315-22341-8

THE UNIVERSITY OF ALBERTA

RELEASE FORM

NAME OF AUTHOR XIAOMAO ZHANG
TITLE OF THESIS FLUID INCLUSION AND STABLE ISOTOPE
STUDIES OF THE GOLD DEPOSITS IN
OKANAGAN VALLEY, BRITISH COLUMBIA
DEGREE FOR WHICH THESIS WAS PRESENTED MASTER OF SCIENCE
YEAR THIS DEGREE GRANTED FALL, 1986 .

Permission is hereby granted to THE UNIVERSITY OF ALBERTA LIBRARY to reproduce single copies of this thesis and to lend or sell such copies for private, scholarly or scientific research purposes only.

The author reserves other publication rights, and neither the thesis nor extensive extracts from it may be printed or otherwise reproduced without the author's written permission.

(SIGNED) *Zhang Xiaomao*

PERMANENT ADDRESS:

Beijing College of Geology
Beijing P. R. China
.....

DATED *June 19* 1986

THE UNIVERSITY OF ALBERTA
FACULTY OF GRADUATE STUDIES AND RESEARCH

The undersigned certify that they have read, and recommend to the Faculty of Graduate Studies and Research, for acceptance, a thesis entitled FLUID INCLUSION AND STABLE ISOTOPE STUDIES OF THE GOLD DEPOSITS IN OKANAGAN VALLEY, BRITISH COLUMBIA submitted by XIAOMAO ZHANG in partial fulfilment of the requirements for the degree of MASTER OF SCIENCE in ECONOMIC GEOLOGY.

B. E. Nesbitt
.....

Supervisor

R. A. Burnham
.....

Leslie H.
.....

Jim Whiting

Date *June 19, 1986*
.....

ABSTRACT

Two kinds of gold mineralization, epithermal and mesothermal, occur in the Okanagan Valley, southern British Columbia. Fluid inclusion and stable isotope studies indicate that two distinctive hydrothermal fluids were responsible for the mineralization events. At Dusty Mac, the epithermal fluid had a temperature of about 240°C, a low salinity of about 0.5 wt% NaCl equivalent and a low value for $\delta^{18}\text{O}(\text{SMOW}) = -7$ to -9 per mil. The mineralization process probably occurred at a depth of more than 380 meters. At Oro Fino and Fairview, the mesothermal fluids had a high CO_2 content, temperatures of 280°-330°C, salinities of 4-6 wt% NaCl equivalent and $\delta^{18}\text{O}(\text{SMOW})$ of $+4$ to $+6$ per mil. The mineralization occurred at a depth of 3-4 km. The data indicate that fluids involved in both mineralization processes originated from meteoric water, with the shallow circulation responsible for the epithermal deposit (Dusty Mac) and deep circulation for the mesothermal ones (Oro Fino and Fairview).

ACKNOWLEDGMENTS

I wish to thank Dr. B. Nesbitt for his patient supervision and guidance in the course of this study. Dr. K. Muehlenbachs generously allowed me to use the facilities for the stable isotope study. I am much obliged for his help in isotope study. Thanks are also given to Mr. D. Rucker for his great help and encouragement during field work. I also acknowledge with gratitude the laboratory help by Mrs. E. Toth. Acknowledgement are due to D. Tempelman-Kluit of GSC for his initial introduction of the gold deposits in Okanagan valley. Lab help and suggestions of Dr. J. Murowchick are well appreciated. All the graduate students in Economic Geology Unit, Department of Geology, University of Alberta are thanked for their help during the course of my study.

Table of Contents

Chapter	Page
ABSTRACT	iv
ACKNOWLEDGMENTS	v
1. INTRODUCTION	1
2. PURPOSE OF THIS STUDY	4
3. GENERAL GEOLOGY	6
4. GEOLOGY OF ORE DEPOSITS	9
4.1 Fairview Camp	9
4.2 Oro Fino Camp	12
4.3 Dusty Mac Mine	13
4.4 Mineralization	14
5. FLUID INCLUSION STUDIES	21
5.1 Fluid Inclusion Techniques	21
5.2 Description of Fluid Inclusions	22
5.3 Temperature Measurements	25
5.3.1 Dusty Mac	31
5.3.2 Oro Fino	33
5.3.3 Twin Lake	34
5.3.4 Stemwinder	35
5.3.5 Morning Star	37
5.3.6 Fairview	41
5.4 Pressure-depth estimation	45
6. STABLE ISOTOPIC STUDIES	52
6.1 Techniques	52
6.2 Isotopic Compositions	53
6.2.1 Dusty Mac	53
6.2.2 Fairview Camp	58

6.2.2.1 Oxygen isotopic compositions58
6.2.2.2 Carbon isotopic composition65
6.2.3 Oro Fino Camp67
7. MODEL OF THE MINERALIZATION70
7.1 Epithermal Mineralization70
7.2 Mesothermal Mineralization75
8. CONCLUSIONS AND FUTURE WORK86
REFERENCE88
APPENDIX: SAMPLE LOCATIONS99

List of Tables

Table	Page
1. Microthermometry data.....	27
2. Oxygen isotopic compositions of quartz and rocks from Dusty Mac deposit.....	54
3. Oxygen and carbon isotopic compositions of minerals and rocks from Fairview Camp.....	59
4. Oxygen isotopic compositions of quartz and rocks from Oro Fino Camp.....	68
5. Summary of the characteristics of hydrothermal ore-forming fluids in the Okanagan Valley.....	71

List of Figures

Figure	Page
1. Index map of this study.....	2
2. Geological map of Okanagan Valley.....	7
3. Geology of the Fairview Camp.....	10
4. Type A quartz vein.....	15
5. Type B quartz vein.....	15
6. Type C quartz veins.....	16
7. 2-phase CO ₂ -H ₂ O inclusions.....	23
8. 3-phase CO ₂ -H ₂ O inclusions.....	23
9. 2-phase aqueous inclusions.....	26
10. Histogram of homogenization temperatures of aqueous inclusions from Dusty Mac.....	32
11. Histogram of ice melting temperatures of aqueous inclusions from Dusty Mac.....	32
12. Histogram of homogenization temperatures of CO ₂ phase of CO ₂ -H ₂ O inclusions from stemwinder:.....	36
13. Histogram of homogenization temperatures of CO ₂ -H ₂ O inclusions from stemwinder.....	36
14. Wide range of CO ₂ /H ₂ O ratios in CO ₂ -H ₂ O inclusions.....	39
15. Histogram of homogenization temperatures of CO ₂ phase of CO ₂ -H ₂ O inclusions from Morning Star.....	40
16. Histogram of homogenization temperatures of CO ₂ -H ₂ O inclusions from Morning Star.....	40
17. Histogram of melting temperatures of clathrate of CO ₂ -H ₂ O inclusions from Fairview.....	43
18. Histogram of homogenization temperatures of CO ₂	

2

phase of CO₂-H₂O inclusions from Fairview.....43

19. Histogram of homogenization temperatures of
CO₂-H₂O inclusions from Fairview.....44

20. P-T diagram for pure CO₂ system.....47

21. Combined P-T diagrams for CO₂ and H₂O systems.....48

22. Isochores for H₂O-CO₂-NaCl system.....50

23. Temperature-salinity relationship of the hydrothermal
ore-forming fluids in the Okanagan Valley.....72

24. Oxygen isotopic compositions of the hydrothermal
ore-forming fluids in the Okanagan Valley.....72

25. Idealized cross section for the hydrothermal system
for the formation of Dusty Mac deposit.....74

26A. Idealized cross section showing the detachment zone
and fault system as channels for deep circulation
of meteoric water.....80

26B. Cross section showing the fluid flowed along the
detachment zone from west to east.....80

26C. Tempelman-Kluit's mineralization model.....80

27. pH-log f_{O₂} diagram with Au solubility contours.....83

1. INTRODUCTION

Okanagan valley of southern B.C. was a significant gold producing area in early 1900's. Since the end of last century, there have been intermittent prospecting and mining activities in this area. The three main gold producing camps are Fairview, Oro Fino and Dusty Mac (Fig. 1). The Fairview camp is located about 6 km northwest of the village of Oliver. It includes three mines: Fairview, Stemwinder and Morning Star. All three deposits are quartz-vein type gold deposits. They were mined at the beginning of the century (1900's) for several years and reopened in the 1930's for a few years. The total production (Hedley and Watson, 1945) was 150,000 tonnes of ore, with 17,000 oz of gold and 160,000 oz of silver. The mines were abandoned in 1930's. The Oro Fino camp is located about 10 km northwest of Fairview and consists of two quartz vein gold deposits, Oro Fino and Twin Lake (Hedley and Watson, 1945). Recorded production was 24,000 tonnes of ore, with 9,000 oz of gold and a little of silver. Dusty Mac is located 2 km east of the village of Okanagan Falls. It was discovered in late 1960's (Church, 1969, 1970) and mined during 1975 and 1976. The total production were 93,000 tonnes of ore, with 19,000 oz of gold, 340,000 oz of silver and a little copper and lead (Minister of Mines and Pet. Res., B.C., 1975, 1976). The mine was closed in 1977 and it has been re-examined recently by ESSO (White, 1985).

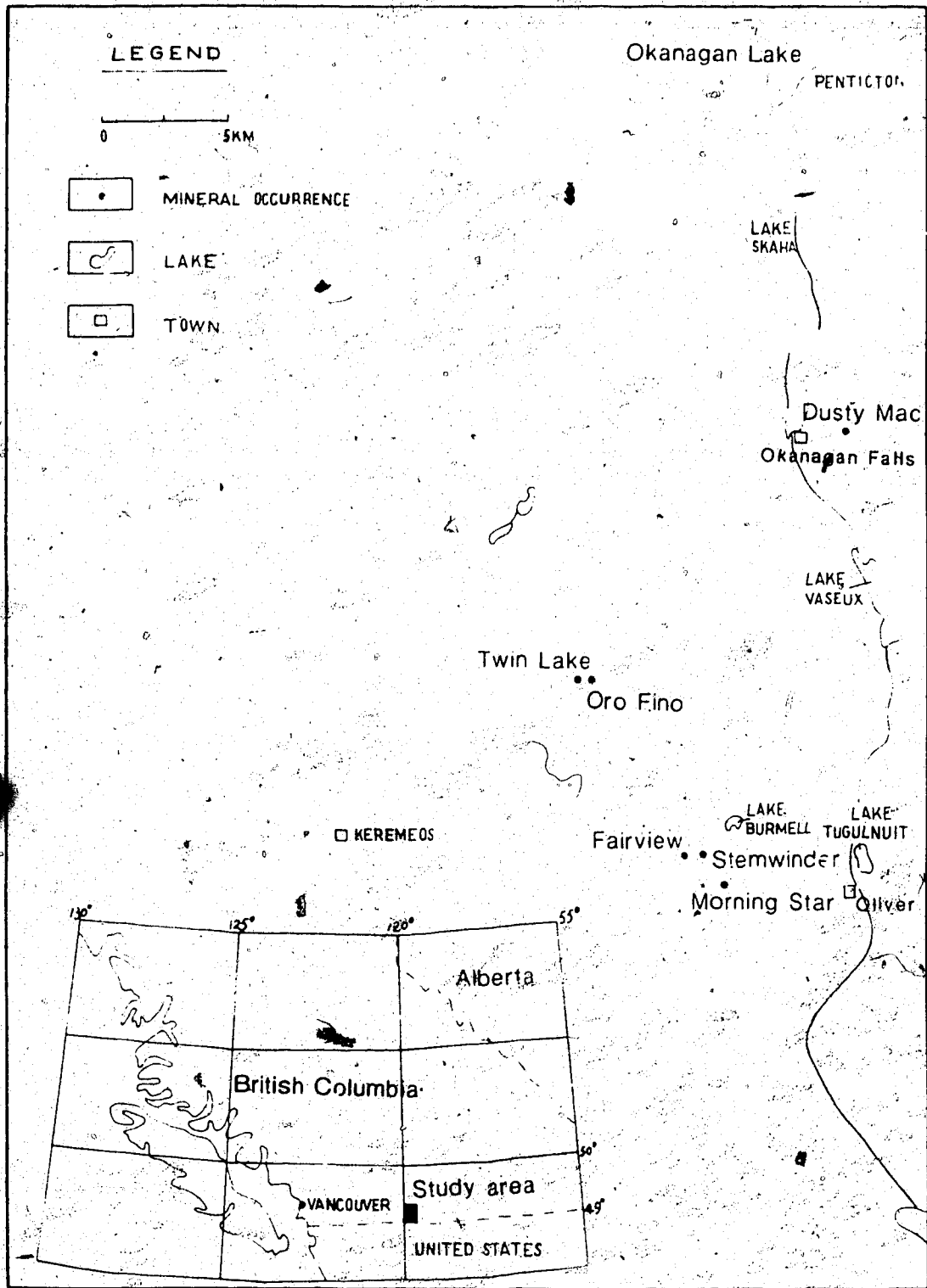


FIG. 1. Index Map of This Study

There is little previous work on the regional geology (Cairnes, 1940; Bostock, 1941; Little, 1961; Church, 1973) and ore deposit geology (Cockfield, 1939; Hedley and Watson, 1945) in this area. Church (1970, 1973) proposed a model of filling of dilations with quartz and Au-Ag mineralization in shear zone for Dusty Mac.

Tempelman-Kluit (1984) proposed a meteoric water model for gold veins in the Okanagan Valley. He suggested that meteoric water flowed through the fault system and leached the metals from the country rocks. When the mineralized fluid discharged, the precious metals deposited above the boiling zone.

2. PURPOSE OF THIS STUDY

There appears to be two different styles of precious metal mineralization in the Okanagan Valley: mineralized quartz veins in metamorphic rocks and silicification zones in the volcanic or volcanoclastic rocks. Both of these styles are believed to have formed by deposition from hydrothermal fluids (Tempelman-Kluit, 1984; Nesbitt et al., in press), but the characteristics and origins of these fluids are still uncertain and the chemical and physical conditions of ore deposition remain to be studied. Nesbitt et al. (in press) have described two distinctive styles of gold deposition, mesothermal and epithermal, in Canadian Cordillera. The two kinds of gold mineralization in the Okanagan Valley provide a good comparison of these two types of mineralization, and may yield interesting results on the origins of the styles of mineralization. In addition, the study of the differing geological and physico-chemical conditions of gold deposition may be a useful tool for exploration for gold in this area.

Since the mines have been abandoned for many years, it is difficult to perform systematical sampling for mineralogical and petrological studies, especially for the mineable part of the deposits. Fortunately, in Fairview mine, a 500 meter adit is still accessible for collecting samples, although more than 50 years have passed.

In order to solve the problems of physical and chemical conditions and origins of the ore-forming hydrothermal fluids, this study compares different gold deposits, through

the studies of stable isotopes and fluid inclusions, as well as the studies of mineralogy and petrology, to obtain information on the characteristics of the ore-forming fluids and the environments of the ore deposition.

In this study, stable isotopic analyses, ^{18}O oxygen and ^{13}C carbon, have been made. About 50 fluid inclusion plates were examined and more than 750 fluid inclusion heating and freezing measurements have been performed. Approximately 100 thin sections and polished sections have been examined.

3. GENERAL GEOLOGY

Tectonically, the Canadian Cordillera is divided into five geological and physiographic provinces (Monger et al., 1979, 1982): Rocky Mountain Belt, Omineca Crystalline Belt, Intermontane Belt, Coast Plutonic Complex and Insular Belt. These belts are believed to have been produced by the accretion of allochthonous terranes to western North America craton at different periods (Monger et al., 1979, 1982; Gabrielse et al., 1982; Price et al., 1985). The Okanagan Valley, located near the boundary between the Omineca Crystalline Belt and Intermontane Belt, follows an Eocene, gently west dipping fault zone, which bounds the west side of a 170 km wide complex (Tempelman-Kluit, 1984) and extends for at least 100 km (Fig. 2). The oldest rocks in this area are gneisses, possibly of Precambrian age. The Paleozoic and Mesozoic successions are also metamorphosed to various degrees. The two major plutons, Okanagan and Valhalla Complexes, intruded the gneisses of Shuswap metamorphic complex. Okanagan batholith is believed to be Jurassic (150-180 Ma) in age (Peto, 1973; Medford, 1975; Peto et al., 1976). Valhalla batholith is younger than the Okanagan batholith. Little (1961) considered Valhalla batholith to be Cretaceous in age, but no exact age-dating is available. Tertiary volcanic and sedimentary rocks dip at comparatively low angles and mainly occur in basin-shaped structures. K-Ar age dating of volcanic rocks yields an Eocene age (45-53 Ma) (Mathews, 1964; Church, 1973). A general

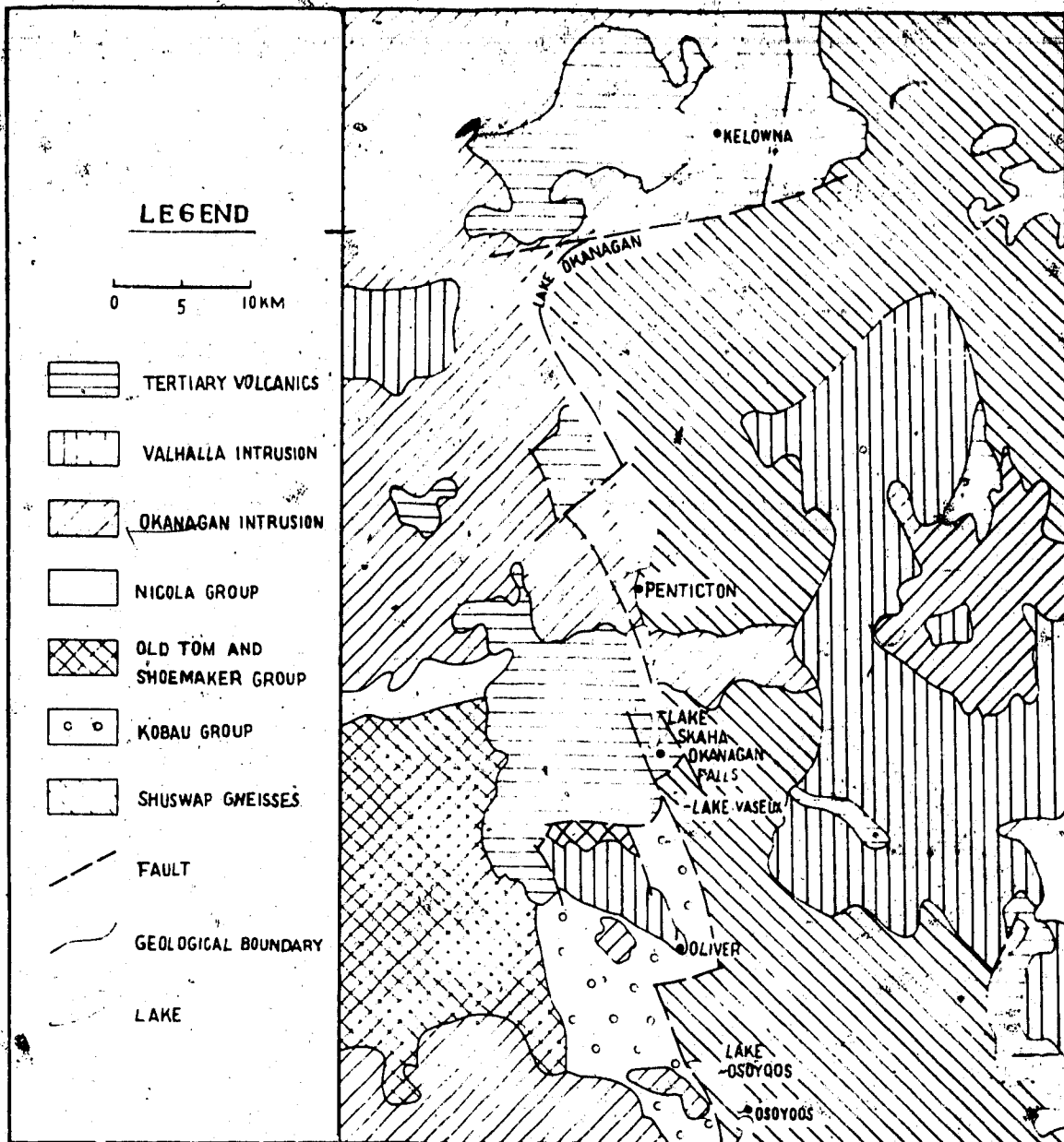


FIG. 2. Simplified geological map of Okanagan Valley area—Sources: Little (1961), Church (1973), Ross et al. (1979), and Parrish et al. (1985)

model for the evolution of the Okanagan area has been developed by Okulitch et al. (1983): the basement was formed at about 1,600 Ma during rifting and received sediments up to late Paleozoic; deformation, minor plutonism and low grade metamorphism occurred during Triassic; in the Jurassic, as the terranes collided with North America, extensive plutonism and metamorphism permeated the region; and, during the Tertiary, extensional tectonism and volcanic extrusion dominated.

4. GEOLOGY OF ORE DEPOSITS

4.1 Fairview Camp

The rocks in the vicinity of the ore deposits are of three groups (Fig. 3). The oldest group is a series of quartz, chlorite, micaceous or graphitic quartz schists of Carboniferous age (Cairnes, 1940). The schists have a pronounced schistosity striking northwesterly ($NW320^{\circ}-350^{\circ}$) and dipping at various angles ($20^{\circ}-40^{\circ}$) to the northeast. The rocks immediately adjacent to the orebodies are micaceous quartz schists or graphitic micaceous quartz schists, which contain high percentage (more than 60 vol%) of quartz. The second rock unit, referred to as the Fairview granodiorite, occurs southwest of the mineralized zone. The rock is coarse grained, with a foliated or gneissic structure. The unit is composed of quartz, andesine, hornblende, micas, and minor epidote and chlorite. It obviously underwent regional metamorphism - the micas, epidote and chlorite are distributed along the foliations. The rock should be classified as gneissic quartz diorite or gneissic granodiorite. The third group, the Oliver granite, consists of light pink to grey, coarse grained rocks and occurs on the northeast side of the ore zone. It contains abundant quartz, potassium feldspar and a little biotite and muscovite. The fact that the Fairview granodiorite possesses a foliated texture and the Oliver granite exhibits a granitic fabric indicates that the former one is older than the last

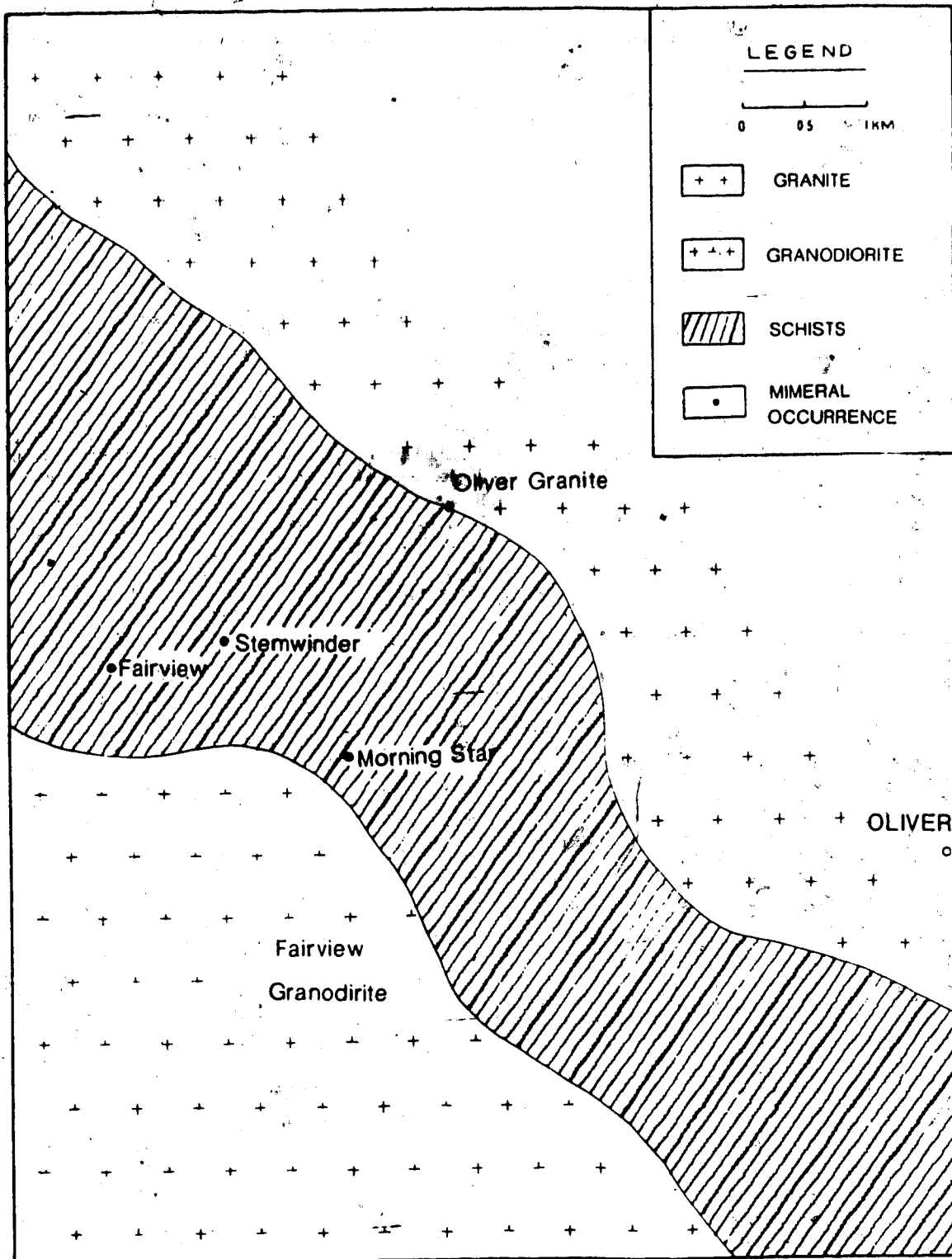


FIG. 3. Geology in the vicinity of Fairview Camp. Revised from B.C. Report of The Minister of Mines, 1933.

metamorphic event, which probably occurred in late Jurassic, and the later one is most likely younger. White et al. (1968) reported K-Ar ages, ranging from 82 to 144 Ma, for Oliver granite, but Medford (1975) stressed that only the oldest K-Ar date could represent the age of the intrusion in this area because the Tertiary thermal event (Rosen, 1975; Medford, 1975) caused partial argon loss.

Numerous quartz veins, generally striking northwesterly with varying widths and lengths, occur in a northwest trending irregular belt about 3-4 km long and 0.5-1.5 km wide (Fig. 3). Three old gold producing mines, Morning Star, Stemwinder and Fairview, follow one or more quartz veins. Figure 3 shows relative positions between them. The Fairview property is situated on a fairly steep slope and is some 1,000 meters west of and about 200 meters higher than the Stemwinder, and about 2,000 meters northwest of and 240 meters above the Morning Star. Two thick quartz veins, known as west and east vein, outcrop on the Morning Star property. Both veins are parallel to the schistosity. The west vein is exposed for about 60 meters along the strike and has a maximum width of about 9 meters. The main workings were on this vein. The main vein of the Fairview conforms to the schistosity and varies considerably in width from less than 1 meter to as much as 6-7 meters. The other two veins, known as north and south vein, were reported (Cockfield, 1939) to have an attitude approximately parallel to the main vein and have a greatest width of 1.5 meters. Cockfield (1939) also reported

that three veins of Stenwinder were probably the continuation of those of Fairview.

4.2 Oro Fino Camp

The country rock is a easterly trending belt of greenstone and highly metamorphosed diorite (Hendley et al., 1945). Based on the observation of this study, the rocks in the vicinity of the ores are amphibolite, gneiss and/or gneissic rocks. They are classified as Triassic units (Bostock, 1941; Little, 1961). These rocks are intruded by dykes of granite and are in fault contact with the Tertiary volcanics. Several quartz veins, discontinuous along strike and with varying dip angles, strike northward or northeastward and have varied widths from 0.5 to 2 meters. Oro Fino and Twin Lake mines follow one or more such veins. Judging from the vein exposed near the entrances of the adits and shafts, the large veins, usually with the width more than 1 meter, have better economic values. An interesting fact is that both mines are situated at almost the same elevation, with a horizontal separation of about 1,000 meters. Two small nameless mines, situated at about 300-400 meters in elevation below the Oro Fino and Twin Lake, also follow such quartz veins.

4.3 Dusty Mac Mine

Dusty Mac is located at the margin of the Tertiary White Lake Basin (Fig. 2). The early Tertiary volcanic rocks, which host the deposit, are composed of five formations. From the oldest to the youngest, they are Springbrook, Marron, Marama, White Lake and Skaha Formations (Church, 1973). The host rock of the ore is the White Lake Formation as described by Church (1969, 1970, 1973), and is composed mainly of feldspar (plagioclase An40-60) porphyry lava, andesitic volcanoclastics, lahars and shale with thin seams of coal in the vicinity of the ore. The older rocks to the immediate west belong to the Marama formation comprising mainly rhyodacite lava. To the east, the White Lake Formation contacts against the old Precambrian Shuswap gneiss. The rocks are on the east limb of a southeasterly trending syncline. The beds have variable dips ranging about 30° to 50° northeast. The rocks are cut by a reverse fault system, which trends generally southeasterly, with interwoven easterly and southerly, and dips northeasterly with an angle of about 40°-50°. The mineralization appears to be largely controlled by the fault system. Quartz veins, silicification zones and gossans are present in or adjacent to the main faults (Church, 1973).

4.4 Mineralization

The gold mineralization in the Okanagan Valley is closely related to the quartz veins or silicification as described above. Limited work on Fairview Camp has shown that three types of quartz veins occur: a) thick quartz veins with one to several meters thick; b) quartz veins with interbedded graphitic bands; and, c) irregular small quartz veins. Type A veins (Fig. 4) are relatively pure quartz veins and are the main ore-bearing veins, as observed at the Fairview deposit. They usually have a thickness larger than 1 meter, and as much as 6-7 meters, with the attitude paralleling the regional schistosity. The quartz is massive, white or milky colour, and has a strong greasy luster. Sulphides are irregularly distributed in the quartz veins as disseminated minerals, small lumps or small veins. The size of type B quartz veins varies. The larger ones may be several meters thick and smaller ones may be 0.1 meter thick. The character of this type of the vein is interbedded white quartz and black graphitic bands (Fig. 5). Generally, the quartz bands are much thicker than the graphitic bands. The quartz of this type looks brittle. Like type A veins, the attitude of type B veins follows the schistosity. Pyrite is sometimes well developed along the graphitic bands, but other sulphides are rare. However, one sample from Morning Star of this type contains a little gold (electrum?) following a small fracture. Type C veins are pure quartz veins with white or glassy quartz. Some small druses occur in this type. The thickness



Fig. 4. Type A quartz vein. The vein is composed of white quartz. Its attitude parallels to the schistosity.



Fig. 5. Type B quartz vein. The graphitic bands are interbedded with thick quartz bands. The vein follows the schistosity.



Fig. 6. Type C quartz veins. The veins cut through the schist at high angles.

of the veins is several centimeters to tens of centimeters. These veins, unlike other two types of veins, cut through the schists at high angles (Fig. 6).

The mineralogy of the orebodies in Fairview Camp is quite simple. Pyrite is the most abundant sulphide and is accompanied by small amounts of galena, sphalerite and chalcopyrite, together with traces of bornite, tetrahedrite, pyrrotite, argentite and boulangerite. There was no report of free gold, but a trace of free gold (element) was observed in fractures in quartz veins in this study. The gold was reported to be principally associated with galena and sphalerite, and not pyrite (B.C. Report of the Minister of Mines, 1933; Hedley and Watson, 1945). Examination of the ore has shown that there are two, possibly three, generations of the quartz. The first generation is the massive milky quartz associated with the pyrite. The second one occurs as small veins associated with other sulphides, usually following the fractures in massive quartz and pyrite. The possible third generation quartz, pure quartz veins, may cut through the above quartz and sulphides. Veinlets of calcite and sericite traversing the quartz (first generation, may be second generation) were also observed. This may be related to the carbonitization and sericitization.

Three distinctive stages of ore mineral deposition can be recognized. Stage 1 is the stage of deposition of milky quartz and pyrite, which usually has a good cubic crystal form. Stage 2 deposited pyrite, chalcopyrite, sphalerite and

minor bornite and pyrrhotite. The well developed exsolution texture of chalcopyrite in sphalerite indicates a relatively high temperature (350°-400°C, Xu, 1982). Stage 3 may be divided into two substages. Stage 3A is a stage of deposition of galena, sphalerite and chalcopyrite following the fractures in the previous minerals. Stage 3B immediately follows the stage 3A. Argentite and boulangierite were deposited and may replace the above minerals during this substage. The small, late, pure quartz veins may be related to stage 3B, but the evidence is inconclusive. Nevertheless, the scarcity of data on gold itself makes it difficult to know during which stage the gold deposited. As mentioned above, if the gold is associated with the galena, it should be deposited at stage 3A.

Except for silicification in the wall rocks, there is no obvious evidence of alteration in hand specimens. However, microscopically, carbonitization, sericitization and chloritization are recognized. Calcite and sericite, either as small veins or disseminated throughout the quartz veins, are related to a later stage of the precipitation of quartz. In some thin sections, their appearance is often associated with pyrite crystals, indicating their relationship with the sulphide deposition. In the vicinity of quartz veins, calcite replaces the metamorphic biotite, muscovite, chlorite and quartz along the schistosity or as small veins in quartz-schist. The late sericite and chlorite also replace the biotite and muscovite along the schistosity. Occasionally

they can replace the carbonate. Alteration does not appear to extend to very far away from the veins. At Morning Star, samples taken from within 50 meters of the main vein show above alterations, but no alteration is observed in samples taken from 100 meters away the main vein.

In Dusty Mac, the mineralized zone is a gently dipping lens of quartz breccia with varying admixture of crushed host rocks. The ore body is about 200 meters long, striking roughly SE140°, with a central cross section width of about 50 meters and maximum thickness of about 10 meters (Church, 1973). The brecciated quartz is of greyish-white colour, but due to the strong chloritization, it shows a greenish-grey colour. The quartz was formed before the structural movement. Numerous small quartz veins, ranging from several millimeters to several centimeters in width, cut through the brecciated quartz and rocks. This quartz is clean and glassy and formed at approximately the same time as the chloritization and carbonitization. Also, from limited studies, the small quartz veins are associated with sulphide mineralization (pyrite and Cu-containing minerals). The metallic minerals, mainly pyrite with traces of chalcopyrite, bornite, galena, sphalerite and native silver (Church, 1970), are disseminated in the breccia zone. Chloritization is intensively developed from the brecciated zone to the host rock. Chlorite forms as aggregates or small veinlets cutting through or pervasively replacing quartz and rock breccias. In addition, carbonitization is also widely developed. Calcite and

calcite-quartz veins may cut through all the other minerals, including chlorite, in the mineral sequence. Clay alteration is also recognized. Several samples show that the clay mineral(s) usually replace the phenocrysts of the rocks.

5. FLUID INCLUSION STUDIES

5.1 Fluid Inclusion Techniques

Quartz samples from each mineral deposit were selected for fluid inclusion studies. The criteria for selecting samples are: 1) quartz which paragenetically relates to ore deposition, and, 2) quartz which represents each type of vein.

Generally, the fluid inclusions studied were very small (usually 5-10 μ m in diameter). The standards used for recognition of the 'primary inclusion' were that the inclusions were distributed individually or in random clusters (Roedder, 1979, 1984; Taylor et al., 1983). Chains of minute inclusions, which are usually less than 1 μ m in diameter and along the healed fractures, were considered to be secondary in origin.

Fluid inclusions were examined in thin (0.3-0.6mm thick), doubly polished plates. Temperature determinations were made using a Chaixmecca heating-freezing stage. The stage was calibrated using standards provided by the manufacturer. Replicate measurements showed that between the range of -60°C and +40°C, the precision was $\pm 0.2^\circ\text{C}$. For higher temperature, homogenization temperatures of the inclusions were reproducible within $\pm 5^\circ\text{C}$, but some inclusions showed a large range of $\pm 10^\circ\text{C}$. Two factors contributed to the difficulty in getting precise homogenization temperatures. First, the optics of the microscope were not adequate for observation at

higher temperature. Secondly, when the inclusion had a dark wall and the vapor bubble contracted against the wall, the exact determination of homogenization was difficult. In the light of the observation, the precision of the homogenization temperatures is estimated as $\pm 5^{\circ}\text{C}$.

The following abbreviations are used: T_h - homogenization temperature of the inclusion; $T_{h\text{CO}_2}$ - homogenization temperature of the CO_2 phase; $T_{m\text{clath}}$ - melting point (disappearance of the last crystal) temperature of the clathrate ($\text{CO}_2 \cdot 5.75\text{H}_2\text{O}$); $T_{m\text{ice}}$ - melting temperature of the ice (H_2O); and, $T_{m\text{CO}_2}$ - melting point temperature of the solid CO_2 .

In this study, room temperature is $24^{\circ}\pm 1^{\circ}\text{C}$.

5.2 Description of Fluid Inclusions

Generally, three types of primary inclusions were recognized, according to the compositions of the fluid inclusions.

Type 1. CO_2 - H_2O inclusions containing CO_2 and aqueous fluids. The existence of the CO_2 phase was confirmed by the fact that the melting temperature of the solid of this phase was around -56.6°C (CO_2 triple point). CO_2 - H_2O inclusions show two phases (CO_2 liquid and H_2O liquid) or three phases (CO_2 liquid, CO_2 vapor and aqueous liquid) at room temperature (Fig. 7 and Fig. 8). For the 2-phase CO_2 - H_2O inclusions, a third phase (CO_2 vapor) forms when cooling the inclusions to about 5°C to 15°C . Without cooling, it is

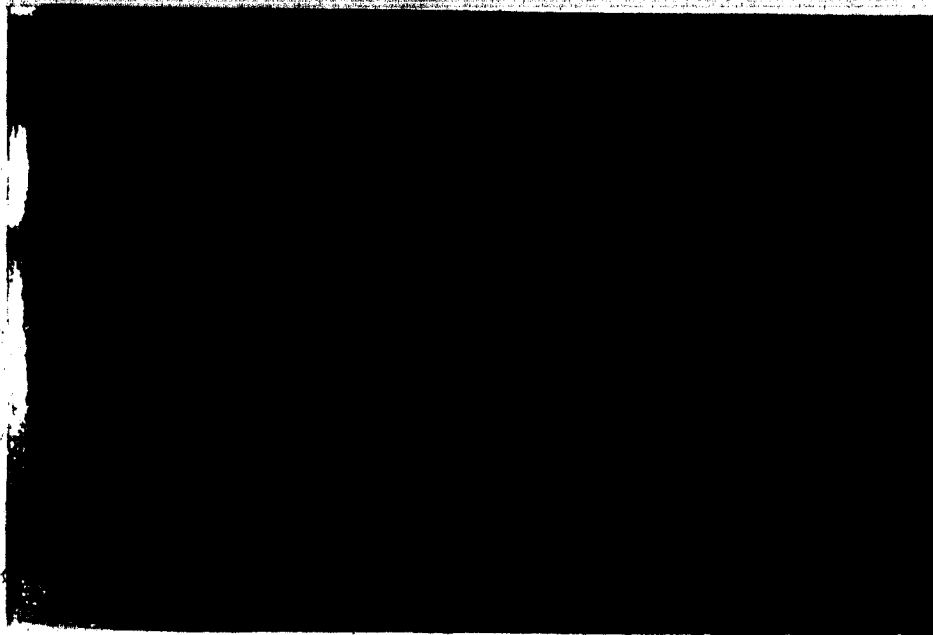


Fig. 7. 2-phase CO₂-H₂O inclusions. Sample F-1.
x500.



Fig. 8. 3-phase CO₂-H₂O inclusions. Sample F-2.
x500.

difficult to distinguish the 2-phase $\text{CO}_2\text{-H}_2\text{O}$ inclusions from the 2-phase aqueous inclusions. For type 1 inclusions, clathrate and solid CO_2 were usually formed at about -30° -40°C and -95° -105°C , respectively. The shapes of type 1 inclusions are variable, from spherical, short prismatic to irregular, with the average diameter of 5 to 10 μm , although some larger inclusions may be 15 μm or more. The CO_2 phase occupies different percentages of the total inclusion volume at different deposits, ranging from 10 to 90 percent, but 20 to 30 percent is more common. Due to high internal pressures, some of the $\text{CO}_2\text{-H}_2\text{O}$ inclusions decrepitated during heating. Heating tests showed that most of the decrepitated inclusions decrepitated at the temperatures just before their homogenization, but some had decrepitation temperatures a little higher (about 20° -30°C) than their homogenization temperatures.

Type 2. CO_2 inclusions containing almost pure CO_2 . At room temperature, the inclusions show one (CO_2 liquid) or two (a CO_2 vapor bubble enveloped by CO_2 liquid) phases. A vapor phase formed when the one phase CO_2 inclusions were cooled. Both one and two phase CO_2 inclusions formed CO_2 solid when the temperature decreased to about -100°C . The solid melted at about -56.6°C . Unlike type 1 inclusions, no clathrate formed in type 2 inclusions. The size of type 2 inclusions is small. Typical diameters for the CO_2 inclusions were 3-5 μm . CO_2 inclusions are closely related to $\text{CO}_2\text{-H}_2\text{O}$ inclusions, especially when the $\text{CO}_2\text{-H}_2\text{O}$ inclusions have a

wide range of filling ratios($\text{CO}_2/(\text{CO}_2 + \text{H}_2\text{O})$). This suggests that the CO_2 inclusions are an end member of the $\text{CO}_2\text{-H}_2\text{O}$ inclusions(type 1 inclusions).

Type 3. Aqueous fluid inclusions containing aqueous vapor and liquid. Most of the type 3 inclusions occurred at Fairview and Oro Fino are similar in size, phase ratio and occurrence to the 2-phase type 1 inclusions. The vapor phase occupies much smaller volume, about 5 to 10, percent of the total inclusion volume at Dusty Mac(Fig. 9).

Secondary fluid inclusions are always present. They might be classified as type 4 inclusion. This type of inclusion is usually distributed along the healed fractures and usually has an elongate shape. The inclusions are very small(usually less than $1\ \mu\text{m}$), with a few exceptions, making it difficult to make heating and freezing measurements. From some measured type 4 inclusions, It is apparent that secondary inclusions were filled with aqueous fluid, but most of them seemed to be only one phase(H_2O liquid?). The secondary inclusions probably belong to several generations.

5.3 Temperature Measurements

Five temperatures: melting temperatures of solid CO_2 , clathrate and H_2O ice and homogenization temperatures of CO_2 and $\text{H}_2\text{O-CO}_2$ or H_2O liquid-vapor were determined. The data are listed in table 1.

Melting of solid CO_2 , clathrate and ice were determined when the jagged margin of vapor phase suddenly disappeared.



Fig. 9. 2-phase aqueous inclusions. Sample
D-14-V. x333.

TABLE 1. MICROTHERMOMETRY DATA

Sample	Mineralogy	Inclusion type	TmCO ₂ Range	Mean	Tmice ^a Range	MAC	Temperature (°C)		ThCO ₂ Range	Mean	Th Range	Mean
							Tmclath Range	Mean				
D-14-V	Qtz	3			-0.3--2.6(11)	-1.5	DUSTY				236-303(13)	264
D-15	Qtz	3			-0.3--1.0(7)	-0.5					131-289(5)	184
D-29-V	Qtz	3			-0.2-0.0(2)	-0.1					116-146(6)	131
D-13	Qtz	3			-0.3--1.0(6)	-0.5					193-295(24)	242
D-28	Qtz	3			-0.2--1.1(7)	-0.4					148-186(3)	163
D-29-B	Qtz	3			-0.6-0.0(5)	-0.3	ORO FINO				168-284(11)	228
O-1	Qtz	1									161-276(19)	215
O-8	Qtz	1			-0.4-0.0(9)	-0.2					204-276(10)	234
O-11	Qtz+py	1									318-349(3)	333
O-12	Qtz+Py	1									197-223(2)	212
T-10	Qtz	1			-56.9--57.3(4)	-57.1					289-323(4)	301
T-11	Qtz	1			-56.7--56.8(2)	-56.8					302-314(2)	308
T-12	Qtz	2			-56.6--57.5(8)	-57.0					246-351(12)	310
S-3	Qtz	1			-57.0--57.3(2)	-57.2					277-343(10)	298
S-8	Qtz	1			-56.5--57.1(5)	-56.9					251-318(3)	278
S-12	Qtz+Py	1			-56.8--58.3(7)	-57.6					264-342(19)	306
TWIN					-56.9--57.2(2)	-57.1					285-303(5)	294
LAKE					-57.0--57.3(2)	-57.2					250-302(7)	270
STEMWINDER					-0.7--2.2(4)	-1.6					160-201(10)	177
STEMWINDER					-5.1--5.7(3)	-5.5					220-328(9)	267
STEMWINDER					6.1-8.5(9)	7.5					229-313(21)	263
STEMWINDER					8.1-9.6(12)	9.0					172-199(4)	186
STEMWINDER					7.6-9.5(16)	8.7					245-320(21)	285
STEMWINDER					-0.3--0.7(2)	-0.5					224-312(31)	258
STEMWINDER											168-238(7)	190

SP-6	Qtz+Sph+Ga 1	-58.0--59.1(4)	-58.5	MORNING	STAR	8.1-9.9(4)	8.6	11.0-15.3(5)	12.6	229-317(25) 4	278
M-16	Qtz+Py+Gr 1 4	-57.0--57.7(7)	-57.3	-1.0--2.7(2)	-1.9	6.9-8.8(9)	7.7	18.0-23.2(11)	20.4	266-312(18)	295
M-29	Qtz 1 2	-56.9--58.9(7)	-58.4			5.6-8.9(8)	7.7	9.8-20.7(7)	14.9	142-150(2)	166
		-57.9--58.4(2)	-58.2					13.1-14.6(2)	13.9	268-332(18)	309
M-35	Qtz 1	-56.7--56.8(2)	-56.8			6.8-7.4(2)	7.1			189-332(16)	266
MP-3	Qtz+Py 2	-57.1--58.3(8)	-57.8			5.8-9.3	7.3	16.1-22.2(9)	19.4	210-322(24)	273
								21.1(1)			
MP-5	Qtz+Py 1 2	-56.8--57.8(5)	-57.1			6.7-8.2(2)	7.5	13.8-21.8(8)	18.0	181-191(2)	186
		-57.1(1)						14.6-19.5(2)	17.1	270-362	309
MP-6	Qtz+Sph +Ga+Py 1	-56.5--57.0(5)	-56.8			8.8-9.4(5)	9.2	27.1-28.9(6)	27.8	178-312(30)	254
MP-12	Qtz+Py 1	-56.9--58.4(7)	-57.4			6.0-7.2(4)	6.6	11.2-22.3(11)	16.4	274-331(14)	303
FA-1	Qtz+Cp+Ga 1	-56.7--58.1(4)	-57.3			7.4-8.9(6)	8.0	18.9-28.6(7)	25.8	185-318(25)	248
	+Sph+Py 2 4	-57.5(1)						26.3(1)			
FA-4	Qtz 1 2	-56.8--57.1(2)	-57.0			5.4-8.5(5)	7.4	24.0-27.8(5)	26.4	190-208(2)	199
		-56.9(1)						26.9(1)		196-333(42)	264
FA-5	Qtz+Ga 1	-56.6--57.0(4)	-56.8			6.6-8.2(4)	7.1	9.3-24.2(7)	18.9	242-303(15)	278
FA-6	Qtz+Ga+Py 1 3 4	-57.1--57.3(2)	-57.2			7.3-7.7(2)	7.5	26.1-27.8(3)	26.7	210-320(19)	273
										275(1)	
										150(1)	
FA-13-V	Qtz 1	-57.4--57.6(2)	-57.5			7.8-8.1(3)	7.9	18.5-28.0(22)	24.7	194-328(29)	275
FA-14	Qtz 1	-56.6--56.8(4)	-56.7			7.0-8.4(4)	7.7	19.7-27.7(3)	24.5	208-324(31)	266
FA-18	Qtz+Gr 1 2	-56.7--57.3(4)	-57.0			6.9-8.4(6)	7.6	16.6-28.4(11)	22.7	210-328(19)	257
		-57.2(1)						20.6(1)			
FA-21	Qtz+Py+Gr 1					6.7-7.7(5)	7.3	20.8-26.2(8)	24.2	261-308(8)	287
FA-24	Qtz+Py 1 3	-56.9--57.3(7)	-57.1			6.8-9.2(7)	7.5	13.3-28.8(7)	19.6	230-296(11)	268
										313(1)	
FA-30	Qtz+Ga+Py 1 4					6.8-7.9(7)	7.4	9.3-27.9(8)	22.8	215-293(9)	267
F-1	Qtz 1	-57.0--57.2(3)	-57.1			6.5-8.2(3)	7.5	19.3-27.1(5)	23.4	146-211(5)	189
F-2	Qtz 1	-57.3(1)				7.5-8.7(2)	8.1	12.5-29.2(11)	22.6	204-320(22)	284
										197-320(27)	275

FAIRVIEW

F-3	Qtz	1	-56.9--57.2(4)	-57.1	6.4-7.8(4)	7.1	21.3-28.0(10)	25.5	215-319(22)	272
F-4	Qtz	1	-57.6--57.7(2)	-57.7	8.7-9.1(2)	8.9	27.8-28.3(4)	28.1	247-306(7)	278
F-6	Qtz	1							263-342(11)	301

1. Numbers in parentheses are the numbers of the measurements.

2. Inclusion types: 1) CO₂-H₂O type, 2) CO₂ type, 3) aqueous type, 4) secondary type.

3. Abbreviations: Cp = chalcopyrite, Ga = galena, Gr = graphite, Py = pyrite, Qtz = quartz, Sph = sphalerite.

and a spherical vapor bubble formed. Homogenization of CO_2 and $\text{H}_2\text{O}-\text{CO}_2$ or H_2O vapor-liquid were determined when the boundary of two distinct fluid phases disappeared. Most of the fluids homogenized to liquid phase.

Most of the CO_2 -containing inclusions (type 1 and type 2) have melting temperatures of solid CO_2 ranging from -56.5°C to -58.5°C (table 1). This implies that these inclusions contain essentially pure CO_2 (Hollister et al., 1976; Burrus, 1981a, 1981b). Nevertheless, depression of melting temperature of solid CO_2 in some inclusions indicates the existence of some other gas(es), probably CH_4 . According to Swanenberg (1979), at the degree of filling of 0.2-0.3 (most common in CO_2 - H_2O inclusions from Oro Fino and Fairview), the melting temperature of CO_2 of -57.5°C indicates a CH_4 content of about 5 percent in the CO_2 - CH_4 system. Since most of the measurements of $T_m\text{CO}_2$ are higher than -57.5°C (table 1), it is concluded that the CO_2 phase in most of the inclusions here is essentially pure CO_2 .

Salinity determinations were based on freezing point depressions of ice in the system of $\text{H}_2\text{O}-\text{NaCl}$ (Potter et al., 1978) for aqueous inclusions and depressions of the decomposition of clathrate in the system of $\text{H}_2\text{O}-\text{CO}_2-\text{NaCl}$ for CO_2 - H_2O inclusions (Bozzo et al., 1973; Collins, 1979). Although the exact value of the melting temperature of CO_2 hydrate is questioned by some authors, e.g., Roedder (1984), it nevertheless gives an estimate. Since the CO_2 phase studied here is essentially pure, the influence of other

gases on melting temperature of clathrate is small.

Densities of CO_2 were based on the table of Amagat (in He Zhi, 1980), which gives the experimental data for liquid-vapor saturation curve for CO_2 . By measuring homogenization temperature of the CO_2 , the densities of CO_2 were obtained.

Homogenization temperatures were not corrected for pressure at this stage.

5.3.1 Dusty Mac

Both brecciated and vein quartz contain a few aqueous inclusions. The inclusions are usually small in size with some larger inclusions ranging up to 10 to 15 μm . The vapor bubble occupies only about 5 percent of the inclusion volume in samples from brecciated quartz, but about 10 percent for samples from vein quartz. The results (table 1) show that the properties of the inclusions are basically the same between two kinds of quartz. As a consequence, we can statistically consider them together as a whole.

Homogenization temperatures of primary inclusions range from 161°C to 303°C , with the average of individual samples from 215°C to 264°C . A histogram of homogenization temperatures (Fig. 10) shows a peak at 245°C , compared with the average of 95 inclusions of 233°C . Melting temperatures of ice range 0.0°C to -2.6°C . This gives a salinity of 0.0 to 4.3 wt% NaCl equivalent. Histogram of melting temperatures of ice (Fig. 11) shows a peak at -0.3°C , which corresponds to a

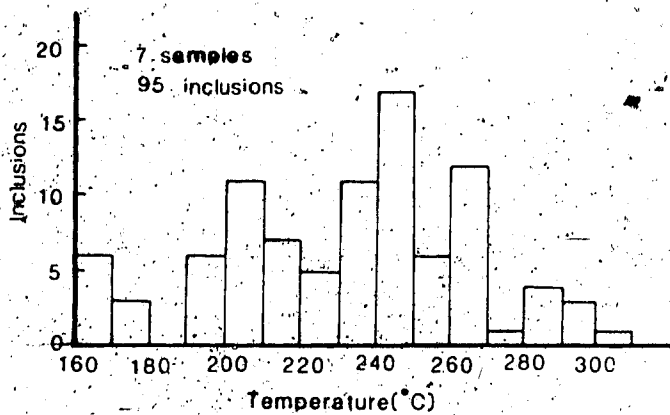


Fig. 10. Histogram of homogenization temperatures of aqueous inclusions from Dusty Mac. The mode is at 245°C.

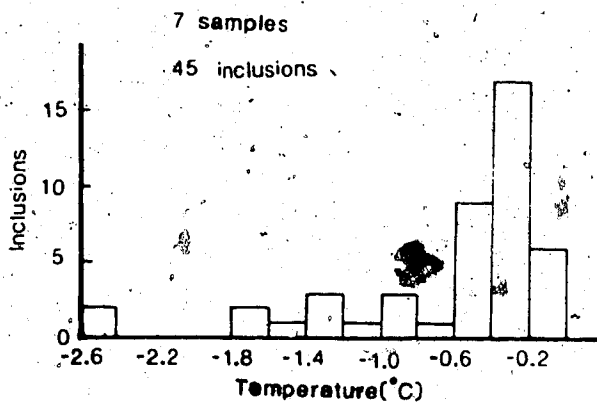


Fig. 11. Histogram of ice melting temperatures of aqueous inclusions from Dusty Mac. The mode is at -0.3°C, which corresponds to a salinity of 0.5 wt% NaCl equivalent.

salinity of 0.5 wt% NaCl equivalent.

Only a few of the secondary inclusions were large enough for measurement. Their homogenization temperatures range from 116°C to 209°C.

5.3.2 Oro Fino

The samples of Oro Fino and Twin Lake deposits used for the study were collected from the veins near the main shafts and waste dumps.

Both CO₂-H₂O and aqueous inclusions were observed in the samples from Oro Fino, but the CO₂-H₂O type dominates. The inclusions are generally smaller than 10 μm. At room temperature, the CO₂-H₂O inclusions usually show three phases (liquid H₂O, liquid CO₂ and vapor CO₂). The CO₂ phase is about 10 to 30 volume percent of the inclusion. The vapor bubbles of aqueous inclusion occupy a similar percentage of the volume.

Homogenization temperatures of the CO₂ phase range from 27.0°C to 30.9°C, with the average of 29.4°C. This gives a CO₂ density of 0.62 g/cm³. The range of melting temperatures of clathrate is from 5.5°C to 8.1°C and the corresponding salinity ranges from 3.8 to 8.3 wt% NaCl equivalent. Average melting temperature of clathrate of 6.4°C corresponds to a salinity of 6.8 wt% NaCl equivalent. Homogenization of H₂O-CO₂ varies from 277°C to 349°C, with an average of 305°C.

Determinations of the depression of the freezing point of aqueous inclusions range from 0.0°C to -0.4°C (sample #

0-11), which is equivalent to 0.0 to 0.7 wt% NaCl. This is somewhat lower than that measured for CO₂-H₂O inclusions. Homogenization temperatures of aqueous inclusions range from 246°C to 351°C, with an average of 304°C.

Three secondary inclusions have the homogenization temperatures of 197°C to 227°C, with an average of 212°C.

5.3.3 Twin Lake

The characteristics of inclusions from the Twin Lake deposit are very similar to that of Oro Fino, but a few CO₂ inclusions were observed at Twin Lake.

For CO₂-H₂O inclusions, melting temperatures of clathrate are from 4.8°C to 8.3°C, which is equivalent to 3.4 to 9.4 wt% NaCl equivalent. The average melting temperature of clathrate of 6.5°C corresponds to a salinity of 6.6 wt% NaCl equivalent. The average homogenization temperature of 27.4°C for the CO₂ phase gives a CO₂ density of 0.66 g/cm³. The total homogenization temperatures range from 264°C to 342°C, with an average of 307°C.

Sample T-11 gives an average melting temperature of ice for aqueous inclusions of -0.7°C, but the sample T-12 gives an average of -5.5°C. Two temperatures indicate salinities of 1.2 and 8.6 wt% NaCl equivalent, respectively. Homogenization temperatures of aqueous inclusions range from 195°C to 301°C, with the average of 246°C.

Two CO₂ inclusions in sample T-11 have melting temperature of solid CO₂ at -57.2°C and homogenization

temperature of 28.5°C, which corresponds to CO₂ density of 0.64 g/cm³.

Several secondary inclusions in sample T-11 have homogenization temperatures ranging from 160°C to 201°C, with an average of 177°C. The average ice melting temperature and salinity were -1.6°C and 2.7 wt% NaCl equivalent, respectively.

5.3.4 Stemwinder

Samples of Stemwinder deposit are from different sites around the mine. S-3 is from a large barren quartz vein about 100 meters away the main shaft. S-8 and S-12 are from the vein at the entrance of the shaft. SP-6 is from a waste dump and may originally have been from the ore-body. All the samples contain numerous small CO₂-H₂O inclusions with a size of 5-10 μm. At room temperature, most of this type of inclusions show two phases (H₂O liquid + CO₂ liquid). A CO₂ vapor is present in some inclusions. The degree of filling of CO₂ (CO₂/(CO₂ + H₂O)) varies from 10 to 60 percent in volume, but in most of the inclusions, CO₂ occupies about 20 percent of the total inclusion volume.

Melting temperatures of clathrate range from 6.1°C to 9.6°C, with most of the measurements clustering around 8.5°C. The salinity, based on the average melting temperature of clathrate (8.5°C), is 3.0 wt% NaCl equivalent.

Homogenization temperatures of CO₂ vary from 8.9°C to 27.6°C. Most of them occur at about 25°C (Fig. 12). This

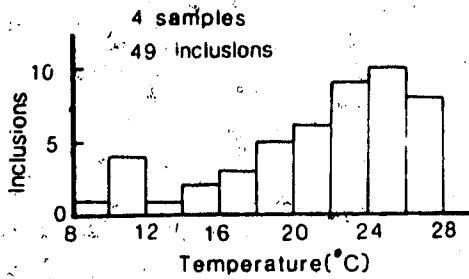


Fig. 12. Histogram of homogenization temperatures of CO_2 phase of $\text{CO}_2\text{-H}_2\text{O}$ inclusions from Stemwinder. The mode is at 25°C .

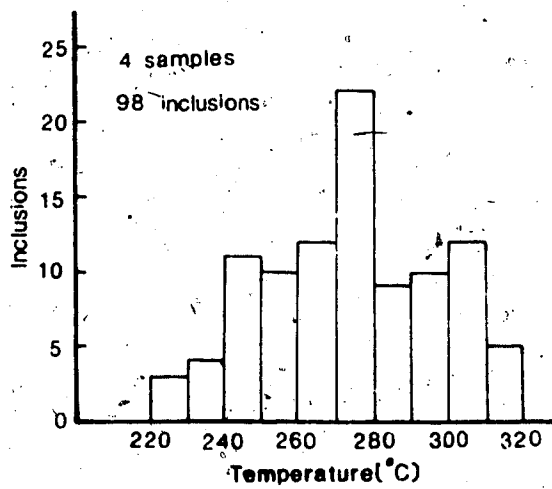


Fig. 13. Histogram of homogenization temperatures of $\text{CO}_2\text{-H}_2\text{O}$ inclusions from Stemwinder. The mode is at 275°C .

corresponds to a CO_2 density of 0.70 g/cm^3 .

The range of total homogenization temperatures is from 224° to 332°C , with the individual sample means from 258°C to 285°C . The histogram (Fig. 13) of homogenization temperatures shows the mode at about 275°C . The average homogenization temperature of 270°C is consistent with this result.

A CO_2 inclusion was measured and the results are $T_{m\text{CO}_2}$ of -56.5°C and $T_{h\text{CO}_2}$ of 12.9°C . This gives a higher CO_2 density of 0.83 g/cm^3 . Since there was only one measurement, the value is somewhat uncertain.

Determinations of secondary inclusions give a range of homogenization temperatures from 169°C to 237°C , with the average of 189°C , and the salinity of 0.9 wt% NaCl equivalent.

5.3.5 Morning Star

At Morning Star, almost all the inclusions observed belong to $\text{CO}_2\text{-H}_2\text{O}$ type. Only a few of CO_2 inclusions were noted. They are closely associated with the $\text{CO}_2\text{-H}_2\text{O}$ inclusions, especially with those inclusions with high CO_2 degrees of filling.

Seven samples from Morning Star were measured. Samples M-16, M-29 and M-35 were from west vein near the entrance of the main shaft. Samples MP-3 through MP-12 were from dump piles and some of them may represent the ore-body.

Numerous small ($3\text{-}10 \mu\text{m}$) $\text{CO}_2\text{-H}_2\text{O}$ inclusions were randomly distributed. At room temperature, the inclusions showed two

phases (liquid H_2O + liquid CO_2), but some 3-phase CO_2 - H_2O inclusions exist in sample MP-6. Degrees of filling by CO_2 varied considerably, from 10 to 90 percent of inclusion volume, even within the same field of view (Fig 14). This phenomenon indicates that a heterogeneous trapping of the fluid might have happened.

Measurements (table 1) show that the inclusions in the two groups of samples (from west vein and from dump piles) are basically similar, in terms of the characters of the fluid.

Melting temperatures of clathrate range from $5.6^\circ C$ to $9.4^\circ C$. This is equivalent to salinities from 1.2 to 8.1 wt% NaCl equivalent. The average melting temperature of clathrate of $7.7^\circ C$ corresponds to a salinity of 4.5 wt% NaCl equivalent. Homogenization temperatures of CO_2 phase vary from $9.8^\circ C$ to $28.9^\circ C$, with a mode at about $21^\circ C$ (Fig. 15) and this indicates a CO_2 density of 0.76 g/cm^3 . The range of total homogenization temperatures was from $178^\circ C$ to $362^\circ C$. As to individual samples, M-35 and MP-6-1 have the largest temperature intervals, from $189^\circ C$ to $332^\circ C$ and $178^\circ C$ to $312^\circ C$, respectively. Two possible factors may be responsible for this behavior: 1) effervescence causing heterogeneous trapping of the fluid; and 2) two generations of inclusions. Since all of the inclusions measured are believed to be primary in origin, the second possibility can be excluded. Thus the most probable reason for the large interval of homogenization temperatures is effervescence of CO_2 . This is consistent with the phenomenon of variable of CO_2/H_2O ratios

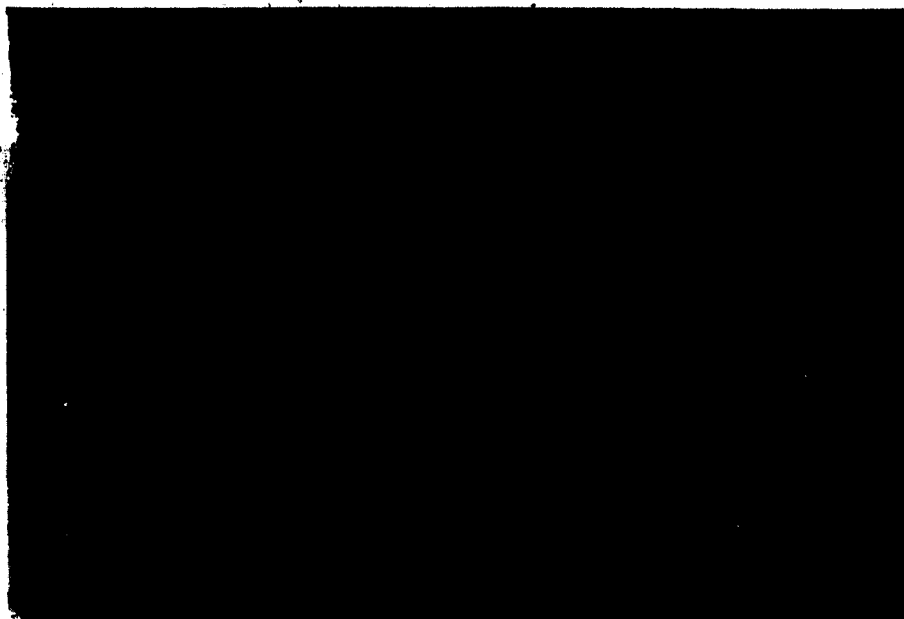


Fig. 14. Wide range of $\text{CO}_2/\text{H}_2\text{O}$ ratios, from less than 20% to more than 80%, in 2-phase $\text{CO}_2\text{-H}_2\text{O}$ inclusions. Sample M-16. $\times 800$.

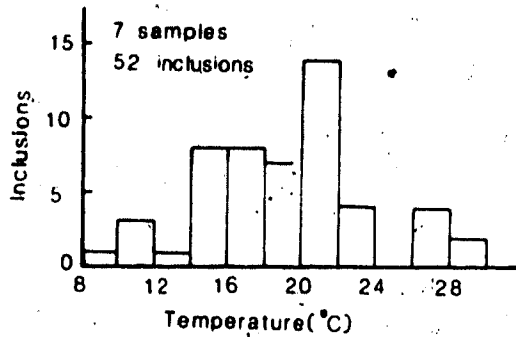


Fig. 15. Histogram of homogenization temperatures of CO_2 phase of $\text{CO}_2\text{-H}_2\text{O}$ inclusions from Morning Star. The mode is at 21°C .

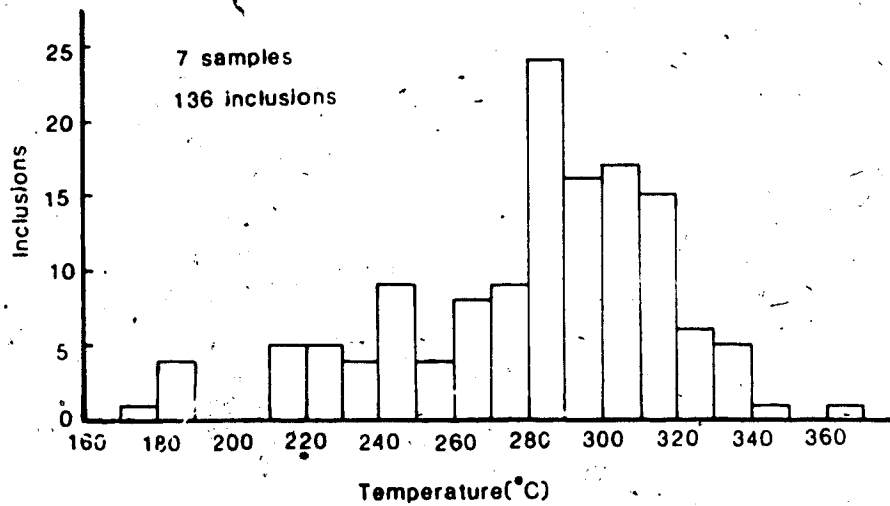


Fig. 16. Histogram of homogenization temperatures of $\text{CO}_2\text{-H}_2\text{O}$ inclusions from Morning Star. The mode is at 285°C .

in this type of inclusions. Measurements of 136 inclusions show that the mode of homogenization temperature is at about 285°C (Fig. 16), compared with the average of 136 inclusions of 277°C.

Several measurements on CO₂ inclusions show melting temperatures of solid CO₂ from -57.5°C to -58.4°C, and homogenization temperatures of CO₂ from 13.1°C to 21.1°C, which corresponds to CO₂ densities of 0.76-0.83 g/cm³.

Two measurements on ice melting temperature for secondary inclusions on sample M-16 give melting temperatures between -1.0 and -2.7°C and the salinity between 1.7 and 3.9 wt% NaCl equivalent. Homogenization temperatures of secondary inclusions range from 142°C to 191°C.

5.3.6 Fairview

Fifteen samples, representing three types of quartz, were used for fluid inclusion studies. Among them, samples F-1 through F-6, FA-1 through FA-6 and FA-30 are from type A veins (FA-1 through FA-6 and FA-30 are from ore-body); samples FA-18 through FA-24 represent type B veins; and, FA-13 and FA-14 represent type C veins.

All four types of inclusions exist in the samples from Fairview, but the CO₂-H₂O type is the most abundant. The average size of the CO₂-H₂O inclusions is about 5-10 μm, but some larger inclusions are as large as 20 μm. Most of the CO₂-H₂O inclusions were three phases (liquid H₂O, liquid CO₂ and vapor CO₂) at room temperature. The CO₂ phase occupied

from 10 to 50 percent of the total inclusion volume, but 20-30 percent was most common.

Measurements show that $\text{CO}_2\text{-H}_2\text{O}$ inclusions from three types of vein quartz have very similar CO_2 densities, salinities and homogenization temperatures (table 1). Variance analysis on homogenization temperatures of $\text{CO}_2\text{-H}_2\text{O}$ inclusions from three types of quartz veins shows that there is no significant difference between them. As a consequence, inclusions from three types of quartz were considered statistically as a whole.

Melting temperatures of clathrate vary from 5.4°C to 9.2°C , and thus the salinities vary from 1.6 to 8.4 wt% NaCl equivalent. The mode of 62 measurements on melting temperature of clathrate is at about 7.7°C (Fig. 17), compared with the average of 7.6°C . This gives a salinity of 4.7 wt% NaCl equivalent. Homogenization temperatures of CO_2 phase are widely distributed (Fig. 18), from 9.3°C to 29.2°C . Figure 18 shows a mode at about 27°C . This temperature is about 3°C higher than the average of 111 inclusions. The corresponding density of Th_{CO_2} of 27°C is 0.67 g/cm^3 . Like Morning Star the homogenization temperatures of $\text{CO}_2\text{-H}_2\text{O}$ inclusions have a large range, even in an individual sample (e.g., FA-4 from 196°C to 333°C , FA-13-V from 194°C to 328°C and F-2 from 197°C to 320°C). This might also indicate the occurrence of heterogeneous trapping of the fluid. However, a histogram of homogenization measurements of 307 inclusions (Fig. 19) shows a mode at about 275°C , compared with the average of 270°C .

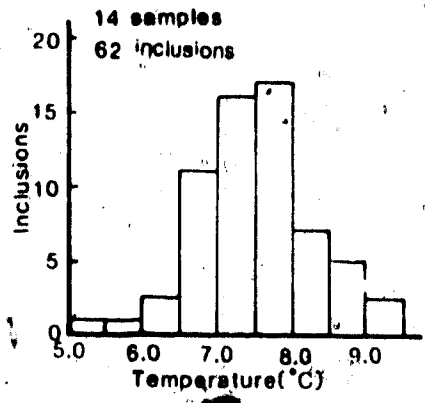


Fig. 17. Histogram of melting temperatures of clathrate of CO₂-H₂O inclusions from Fairview. The mode is at 7.7°C.

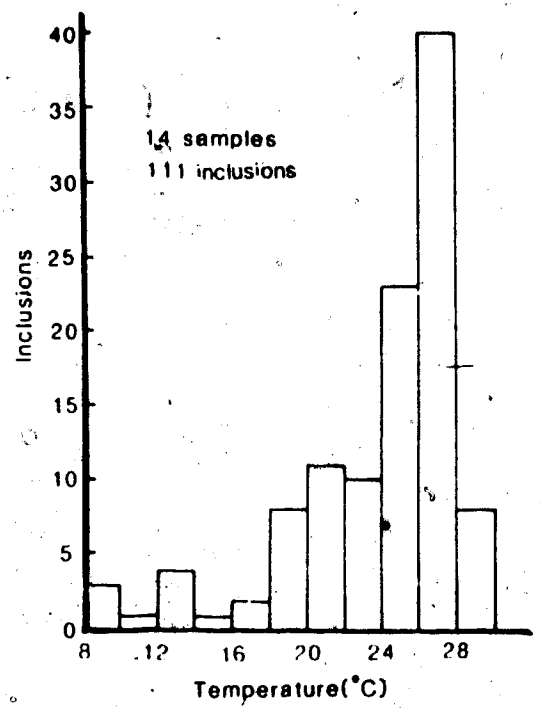


Fig. 18. Histogram of homogenization temperatures of CO₂ phase of CO₂-H₂O inclusions from Fairview. The mode is at 27°C.

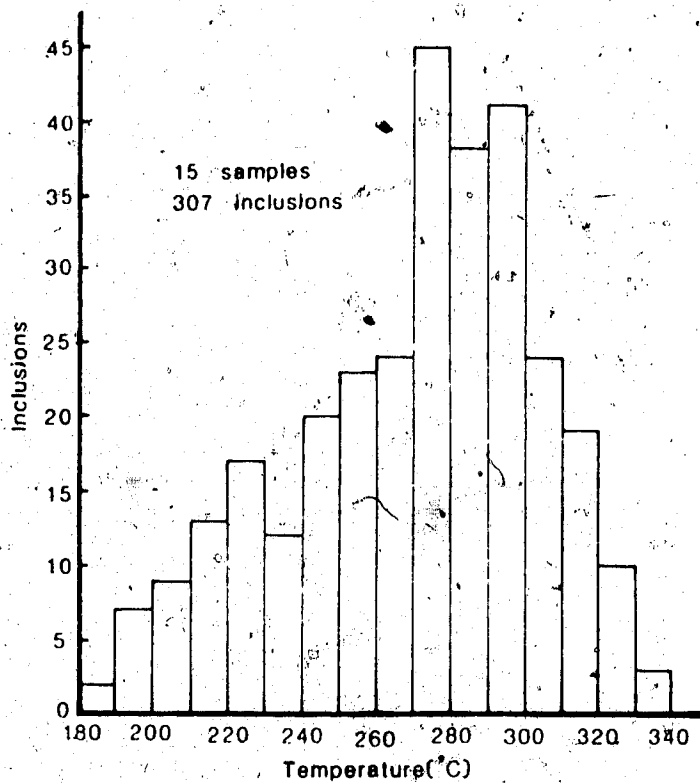


Fig. 19. Histogram of homogenization temperatures of $\text{CO}_2\text{-H}_2\text{O}$ inclusions from Fairview. The mode is at 275°C .

Several CO₂ inclusions show that they have a relatively pure CO₂ composition (triple point temperature -56.9°--57.5°C) and a similar CO₂ density to those of the CO₂-H₂O inclusions.

Since the aqueous inclusions were rare, only a few measurements were done. Two samples show salinities of 2.7 to 4.6 wt% NaCl equivalent and homogenization temperatures of 275° to 313°.

Homogenization temperatures of secondary inclusions range from 150°C to 211°C.

5.4 Pressure-depth estimation

No exact determination of pressure can be obtained from Dusty Mac, but an estimation of vapor pressure by using Hass's data (1971, 1976) for H₂O-NaCl system can give some information about pressure. At Dusty Mac, as shown above, the fluids have very low salinities and are essentially pure water. Assuming pure water, at homogenization temperature of 240°C, the minimum vapor pressure is 34 bars which corresponds to a depth of 380 meters, assuming a hydrostatic pressure gradient, or 120 meters, assuming a lithostatic pressure gradient. This pressure is only a minimum estimate, since the fluid inclusions show no evidence of boiling. Existence of faulting systems, pervasive water/rock interaction (see next chapter) and very low salinity at Dusty Mac suggest that the vein system was open to the surface, and the pressure gradient was hydrostatic. Thus, in the case of Dusty Mac, an approximate minimum trapping depth of 380

meters can be estimated.

The presence of CO_2 inclusions at Twin Lake, Stemwinder, Morning Star and Fairview allows us to determine the fluid pressure in the system. Figure 20 shows the available P-V-T data for CO_2 . As discussed before, CO_2 density at Twin Lake is estimated to be about 0.65 g/cm^3 . At the homogenization temperature of the coexisting CO_2 - H_2O inclusions (taking 300°C as an estimate), the pressure is about 900 bars. Estimation of CO_2 density at Stemwinder, Morning Star and Fairview was about 0.70 - 0.80 g/cm^3 . At homogenization temperature of coexisting CO_2 - H_2O inclusions (taking 275°C as an estimate), the pressure is 980-1320 bars. Using this method, accurate estimation of CO_2 density is very important. For the example above, a density difference of 0.1 g/cm^3 can produce a pressure difference of 340 bars at the measured P-T range. Influence of the temperature on pressure estimate using this method is much smaller: For example, taking the CO_2 density of 0.7 g/cm^3 , the pressure shift is about 100 bars, with the temperature change of 50°C .

Separate CO_2 and aqueous inclusions can be used for geobarometry (Kalyuzhnyi et al., 1953; from Roedder et al., 1980). A few of such situations happened at Twin Lake: In sample T-11, CO_2 inclusions homogenized at 28.5°C and aqueous inclusions at 270°C . This indicates a trapping temperature and pressure of about 330°C and 1,000 bars (Fig. 21), respectively. This pressure is some 100 bars higher than the one above, but is still within reasonable error. The pressure

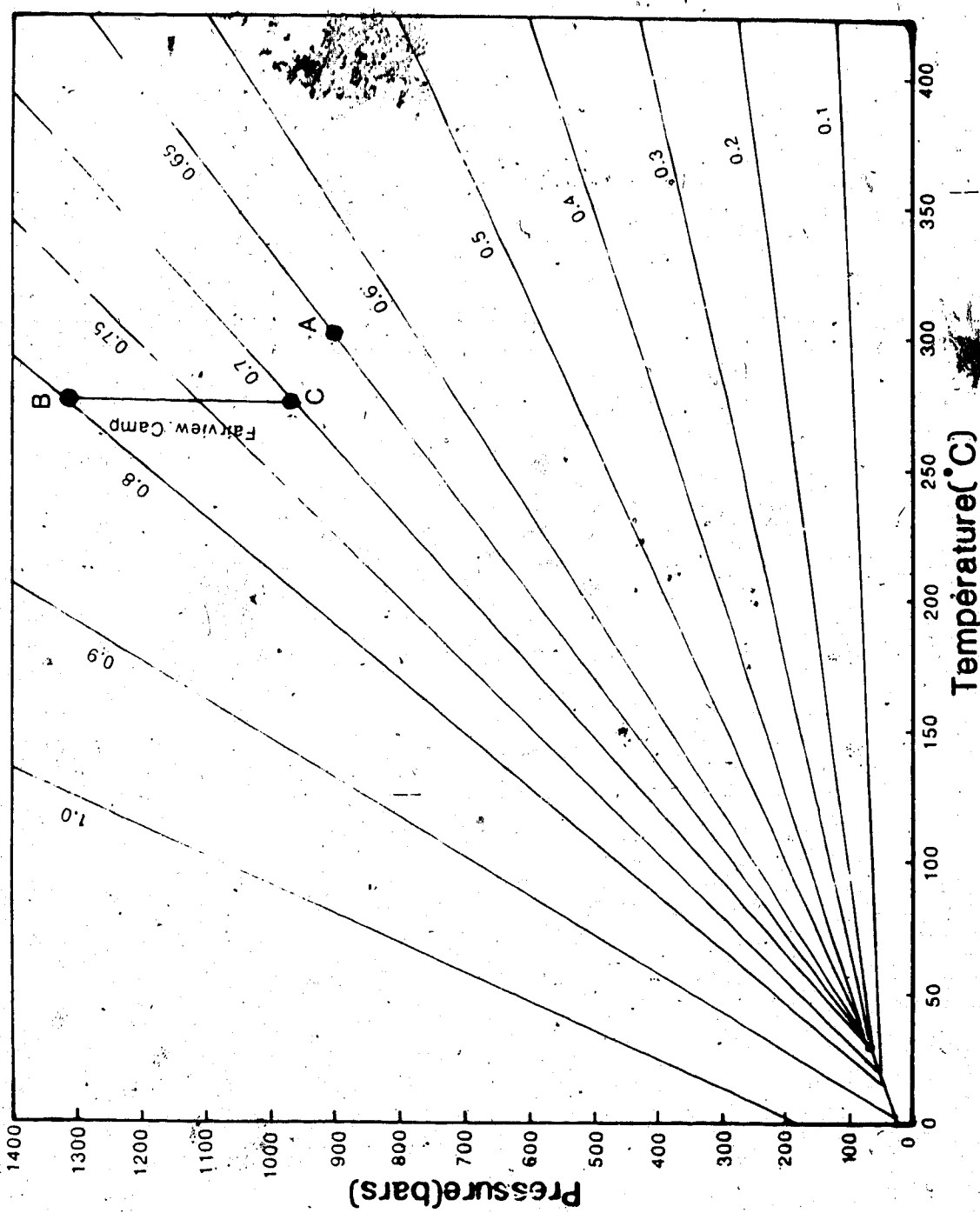


Fig. 20. Combined P-T diagram for the CO₂ system. Solid lines are CO₂ density isopleths. Data are from Kennedy (1954). Point A represents the pressure of 900 bars estimated from CO₂ inclusions from Twin Lake deposit. Line B-C represents the pressure interval of 980-1320 bars estimated from CO₂ inclusions from Fairview Camp.

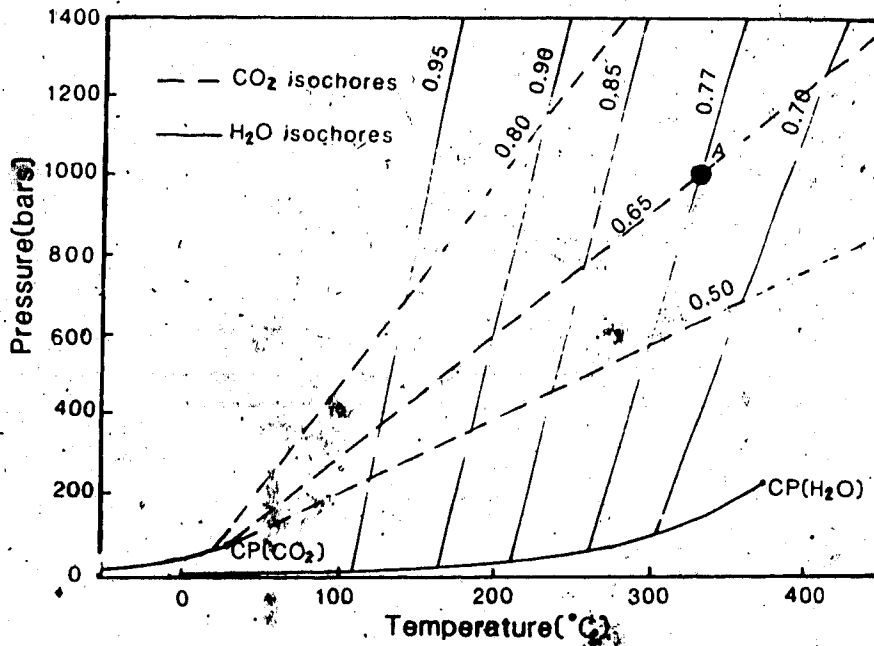


Fig. 21. Combined P-T diagrams for CO_2 and H_2O . Revised from Roedder and Bodnar (1980). Point X represents the common trapping temperature (330°C) and pressure (1000 bars) for CO_2 inclusions homogenizing at 28.5°C (density of 0.65 g/cm^3) and H_2O inclusions homogenizing at 270°C (density of 0.77 g/cm^3).

of 1000 bars corresponds to a depth of about 3600 meters at lithostatic pressure gradient (assuming 275 bars/km).

Bowers and Helgeson (1983a) have calculated P-V-T-X relationship for H₂O-CO₂-NaCl system. Figure 22 shows the isochores and the immiscible area of the solution containing 4.8 wt% NaCl, 20.6 wt% CO₂ and 74.6 wt% H₂O, which is similar to the fluids measured at Fairview area. Assuming heterogeneous entrapment of the fluid occurred at 285°C at Morning Star, the corresponding pressure is about 1150 bars. Since the slope of immiscible curve is steep, temperature drastically influences the pressure obtained using this method. If the temperature is 10°C lower, as the situation at Fairview, the pressure should increase to about 1300 bars to make the solution immiscible. As Fairview is 240 meters higher in elevation than Morning Star, the pressure measured should be somewhat lower than that of Morning Star. The explanation could be the variations of salinity and CO₂ content of the fluid. Salinity can strongly change the solubility of CO₂ in H₂O-NaCl system (Ellis and Golding, 1963; Takenouchi and Kennedy, 1965; Gehrig et al., 1979). A change of the salinity by 0.5 wt% could shift the pressure by about 100-150 bars, at the salinity of about 5 wt% NaCl and the temperature of 285°C, according to Bowers and Helgeson (1983b). On the other hand, increase or decrease of CO₂ content can drastically influence the position of immiscible curve. For example, when the fluid decreases its CO₂ content to 10 wt% CO₂, at same salinity and temperature

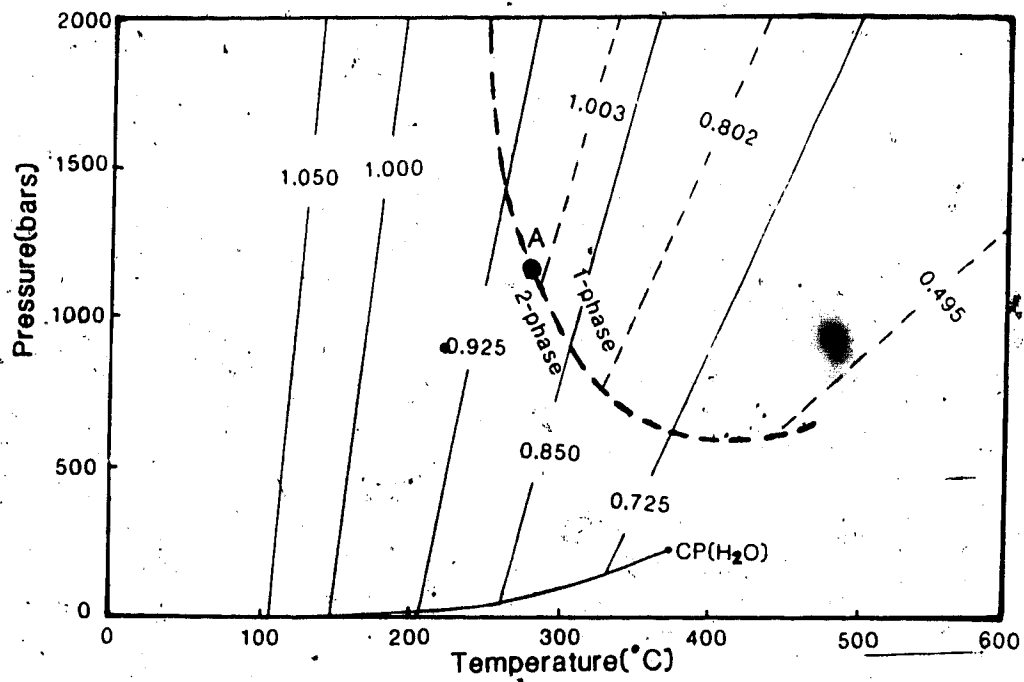


Fig. 22. Isochores for solution compositions corresponding to pure H₂O (solid lines) and 74.6 wt% H₂O, 20.6 wt% CO₂ and 4.8 wt% NaCl (dashed lines). The thick dashed curve is immiscible curve. After Bowers and Helgeson (1983b). Point A represents the trapping temperature and pressure of 285°C and 1150 bars, respectively, for CO₂-H₂O inclusions from Morning Star.

as above, the immiscible curve should be at about 500 bars (Bowers and Helgeson, 1983b).

As discussed above, various methods used for estimation of the pressures give a range from 950 to 1300 bars for Fairview area. Because fluid inclusion studies have shown that the fluids in Fairview area were effervescing when they were trapped, the pressure obtained here should be their "true" trapping pressure. Taking 1100-1200 bars as an estimate for the pressure of mineralization in this area, the corresponding depth is 3900-4300 meters at lithostatic pressure gradient (assuming 275 bars/km).

6. STABLE ISOTOPIC STUDIES

6.1 Techniques

In recent years, numerous stable isotope studies have shown that they are powerful tools in understanding the origins of hydrothermal fluids and ore deposition (e.g., Sugisaki, 1971; Taylor, 1974, 1979; O'Neil et al., 1974; and many others). During this study, the oxygen and carbon isotope values of samples from the various deposits were analysed to determine the isotopic characteristics of the minerals, rocks and hydrothermal fluids.

Carbon isotopic determinations were made on the fluids released from the fluid inclusions and calcite. Oxygen isotopic compositions were made on minerals and rocks.

Most of the samples selected for isotopic analyses were used for fluid inclusion studies. Except some pure quartz samples, all the mineral samples were treated with pure hydrochloric acid at room temperature for one day or more to remove carbonate(s) and then picked under a binocular microscope. The purity of the minerals is better than 95%.

Oxygen was released from quartz, silicates and whole rock samples by reaction with BrF_5 in nickel reaction tubes at about 600°C for 12-14 hours (Clayton et al., 1963), and then converted to CO_2 by the reaction with the hot carbon.

Fluids were extracted from quartz samples by thermal decrepitation. The quartz samples were crushed to a grain size of about 1 mm. The crushed samples were heated to 250°C

in a vacuum line overnight to remove atmospheric water vapor and decrepitate secondary fluid inclusions. The samples were then heated up to 1100°C for 3 hours and the liberated fluid was collected in a liquid nitrogen trap. A dry ice trap was used for separating CO₂ and water vapor. The water vapor was used for hydrogen and the CO₂ for carbon isotopic analyses.

For calcite, the CO₂ was obtained by reaction of the powdered calcite with pure phosphoric acid at 25° for a day (McCrea, 1950).

Oxygen and carbon isotopic compositions were analyzed by using a double collecting, 90° sector mass-spectrometer (Micromass 602D) at the Department of Chemistry, University of Alberta.

For oxygen isotopic analysis, the precision as indicated by replicate analyses on several quartz samples is ±0.2 per mil.

The isotopic compositions of the samples are reported in the δ notation in per mil deviation from SMOW (Craig, 1961) for oxygen and PDB (Craig, 1957) for carbon.

6.2 Isotopic Compositions

6.2.1 Dusty Mac

The $\delta^{18}\text{O}$ values of 7 quartz samples and 6 whole rock samples are summarized in table 2.

The quartz has a narrow $\delta^{18}\text{O}$ range from +0.8 to +2.8 per mil. Oxygen isotopic results show little difference between

TABLE 2. OXYGEN ISOTOPIC COMPOSITIONS OF
QUARTZ AND ROCKS FROM DUST MAC

Sample	Mineral/Rock	$\delta^{18}\text{O}$
D-14-V	Vein quartz	+1.2
D-15	Vein quartz	+1.3
D-29-V	Vein quartz	+0.8
D-8	Brecciated quartz	+2.8
D-13	Brecciated quartz	+2.0
D-28	Brecciated quartz	+1.6
D-29-B	Brecciated quartz	+2.3
D-3	Shale	-1.1
D-4	Andesite	-2.0
D-9	Andesite	-2.7
D-14	Andesite	-1.7
DA-3	Andesite	-0.8
DB-24	Lahar	-3.7

the vein quartz and the brecciated quartz (table 2). This is consistent with the results of the fluid inclusion studies and indicates that the two kinds of quartz have the same origin and similar precipitating environment. It is possible to calculate the oxygen isotopic composition of the water which isotopically equilibrated with the quartz, using the available oxygen isotopic fractionation equation for the quartz-water system. Assuming the quartz was in equilibrium with the fluid at 240°C, using the revised equation of Clayton et al. (1972)

$$10^3 \ln \alpha = 3.38 (10^6 T^{-2}) - 2.90$$

the calculated $\delta^{18}\text{O}$ values of the water range from -7.1 to -9.1 per mil. The average $\delta^{18}\text{O}$ of +1.7 for 7 quartz samples gives a $\delta^{18}\text{O}$ of -8.2 per mil for the water. Increasing the temperature of quartz-deposition by 30°C would shift the calculated $\delta^{18}\text{O}$ value of the water by +1.3 per mil (if the pressure is 250 bars, which should be higher than that of Dusty Mac, pressure correction for homogenization temperature is about 30°C, according to Potter (1977)).

Four whole rock samples (D-3, D-4, D-9 and D-14) from the vicinity of the ore have oxygen isotopic compositions very similar to two samples (DA-3 and DB-24) from about 500 meters away from the ore-body. This indicates that the oxygen isotopic exchange between the fluid and the host rocks was established not only within the vicinity of the ore-body, but also to a considerable distance. The widespread depletion of the $\delta^{18}\text{O}$ in the rocks, about -2.0 per mil at Dusty Mac

comparing with +6.5 per mil of the "normal andesite" (Taylor, 1974), may also indicate that a large amount of low $\delta^{18}\text{O}$ water was involved in water-rock interaction. Of all the possible waters, only meteoric water has a $\delta^{18}\text{O}$ value below zero. Thus, the most probable water involved in water-rock interaction is meteoric water. Taylor (1977) has indicated that during the past 150 Ma the isotopic variation of meteoric waters across North America should have been similar to the present pattern. Present day meteoric water in southern B.C. has $\delta^{18}\text{O}$ values between -13 to -15 per mil. Magaritz et al. (1986) have shown a $\delta^{18}\text{O}$ of -13 per mil for Tertiary meteoric water in the Okanagan area.

Taylor (1974, 1979) has developed a model for calculating the amount of water involved in water-rock interaction as

$$W/R = (\delta_R^f - \delta_R^i) / (\delta_W^i - \delta_R^f + \Delta)$$

where W is the atom percent water oxygen and R is the atom percent rock oxygen in the system, δ^f is the final $\delta^{18}\text{O}$ value and δ^i is the initial $\delta^{18}\text{O}$ value for rocks or waters, and $\Delta = \delta_R^f - \delta_W^f$. Assuming that the $\delta^{18}\text{O}$ value of plagioclase (An30) is approximately equal to the $\delta^{18}\text{O}_r$ at equilibrium (Taylor, 1974), then the oxygen isotope fractionation between plagioclase (An30) and water (O'Neil and Taylor, 1967)

$$\delta^{18}\text{O}_{\text{plag}} - \delta^{18}\text{O}_{\text{water}} = 2.68 \left(\frac{10^6}{T} - 2 \right) = 3.53$$

can be used as Δ for calculating water-rock ratio. Making the reasonable approximations that $\delta_R^i = +6.5$, $\delta_W^i = -13.0$, $\delta_R^f = -2.0$ and $T = 240^\circ\text{C}$, the calculated W/R ratio is 1.9. The above calculation is based on the assumption that no water

escapes from hydrothermal system before isotopic equilibrium has been established. The equation (Taylor, 1979)

$$W/R = \ln \left((\delta_w^i - \delta_r^i + \Delta) / (\delta_w^f - \delta_r^f + \Delta) \right)$$

is used for the open system in which the water passes through the system only once. The calculated water-rock ratio, using the same assumptions as above, is 1.1. The true situation should lie between the two discussed above, i.e., $R/W = 1.1-1.9$. If water-rock ratio is expressed by weight ratio, it should be 0.55-0.95, considering that the rocks only contain 40-50 wt% oxygen, while the water contains 89 wt% oxygen. Assuming the volume of rocks involved in water-rock interaction was at least 0.5 km^3 , the required meteoric water is $0.7-1.4 \times 10^9$ tonnes ($0.7-1.4 \text{ km}^3$ water). This is a large but reasonable number. Oxygen isotopic ratio of the hydrothermal fluid was shifted from the $\delta^{18}\text{O}$ value of meteoric water significantly. Given initial conditions of $T=240^\circ\text{C}$, $\delta^{18}\text{O}_{\text{rock}} = +6.5$, $\delta^{18}\text{O}_{\text{water}} = -13.0$, and $W/R = 1$, the hydrothermal fluid would attain a $\delta^{18}\text{O}$ value of -6.6 per mil under equilibrium condition. The value of -6.6 is higher than the values of -7.1--9.1 per mil obtained from quartz-water fractionation. This is probably because the water-rock ratio is larger than 1 and the oxygen isotopic exchange between the rocks and water was incomplete. If the water-rock ratio is 2, the $\delta^{18}\text{O}$ value of the fluid would be -8.7, using the same conditions. This indicates that the water-rock ratio at Dusty Mac is 1 to 2.

6.2.2 Fairview Camp

The isotopic results from Fairview area are summarized in table 3. The detailed descriptions and discussions on individual isotope are as below.

6.2.2.1 Oxygen isotopic compositions

Thirty-three oxygen isotopic analyses were made on quartz samples from different deposits and different types of veins in the area. They show a narrow range of $\delta^{18}\text{O}$ values, from +11.8 to +14.0 per mil.

At the Fairview deposit, five quartz samples (FA-1 through FA-8) from ore-body have the $\delta^{18}\text{O}$ values from +12.9 to +13.9 per mil. The other five samples of type A vein quartz (F-1 through F-20) show $\delta^{18}\text{O}$ from +11.8 to +13.8 per mil. Four samples of type B vein quartz (FA-18 through FA-24) have the $\delta^{18}\text{O}$ from +13.1 to +13.6 per mil. The $\delta^{18}\text{O}$ values for three samples of type C vein quartz (FA-9 through FA-14) range from +12.4 to +13.6 per mil. A quartz sample (F-32) from a small quartz vein (10 mm wide) in the micaceous quartz-schist about 300 meters northwest of the main entrance has the $\delta^{18}\text{O}$ value of +12.3 per mil. The results show that the oxygen isotopic ratios between three types of quartz veins are almost the same at Fairview. The maximum variation is 2.1 per mil. Using quartz-water fractionation equation (Clayton et al., 1972), the calculated $\delta^{18}\text{O}$ values for the hydrothermal water are from +3.4 to +5.5 per mil, assuming a temperature of 275°C (trapping temperature) for

TABLE 3. OXYGEN AND CARBON ISOTOPIC
COMPOSITIONS OF MINERALS AND ROCKS FROM
FAIRVIEW, MORNING STAR AND STEMWINDER

Sample	Mineral/Rock	$\delta^{18}\text{O}$	$\delta^{13}\text{C}$
Fairview			
F-1	Quartz	+13.6	
F-2	Quartz	+13.8	
F-4	Quartz	+11.8	
F-10	Quartz	+13.6	
F-20	Quartz	+13.5	
F-32	Quartz	+12.3	
FA-1	Quartz	+12.9	
FA-2	Quartz	+13.9	
FA-3	Quartz	+13.4	
FA-4	Quartz	+12.1	
FA-8	Quartz	+12.5	
FA-9	Quartz	+12.4	
FA-13-V	Quartz	+13.5	-8.9
FA-14	Quartz	+13.4	
FA-18	Quartz	+13.6	
FA-19	Quartz	+13.6	
FA-23	Quartz	+13.6	
FA-24	Quartz	+13.1	-8.5
FA-11-Q	Quartz	+13.6	
FA-13-Q	Quartz	+13.0	
FA-13	Micaceous quartz schist	+11.7	
FA-17	Micaceous quartz schist	+14.1	
Morning Star			
M-2	Quartz	+14.0	
M-3	Quartz	+13.3	
M-12	Quartz	+13.6	
M-16	Quartz	+13.4	-8.2
M-29	Quartz	+14.0	
M-35	Quartz	+13.9	
MP-3	Quartz	+13.5	

MP-5	Quartz	+13.9	
MP-6	Quartz	+13.3	
M-5	Micaceous quartz schist	+14.5	
M-6	Micaceous quartz schist	+13.0	
M-6-Q	Quartz	+15.1	
M-7	Micaceous quartz schist	+16.7	
M-7-Q	Quartz	+16.6	
M-7-B	Biotite	+9.5	
M-8	Chlorite schist	+5.7	
M-8-Ch	Chlorite	+5.1	
M-8-V-Q	Quartz	+12.8	
M-8-V-Ca	Calcite	+9.7	-9.1
M-9	Chlorite schist	+8.3	
M-10	Chlorite	+7.0	
	Stemwinder		
S-1	Quartz	+13.2	
S-3	Quartz	+13.3	
S-8	Quartz	+13.3	
S-12	Quartz	+13.2	
SP-6	Quartz	+13.4	

precipitation of the quartz.

At the Morning Star deposit, four quartz samples (M-2, M-16, M-29 and M-35) from the west vein, the main ore producing vein, have $\delta^{18}\text{O}$ values from +13.4 to +14.0 per mil. Three quartz samples (MP-3 through MP-6), picked up from the dump and associated with the sulphide mineralization, have the similar $\delta^{18}\text{O}$ values from +13.3 to +13.9 per mil. Two quartz samples (M-3 and M-12), from east vein about 100 meters east of the main entrance, also have similar $\delta^{18}\text{O}$ values between +13.3 and +13.6 per mil. Sample M-8-V-Q is a quartz sample separated from a small quartz-calcite vein (5 mm wide) in chlorite-schist about 250 meters northeast of the main entrance and gives a $\delta^{18}\text{O}$ value of +12.8 per mil. Maximum variation of the $\delta^{18}\text{O}$ between quartz samples is 1.2 per mil. According to Clayton et al.'s (1972) equation, the calculated $\delta^{18}\text{O}$ of the water between +4.8 to +6.0 per mil, at the temperature of 285°C (trapping temperature).

Five quartz samples from Stemwinder deposit show identical oxygen isotopic composition with $\delta^{18}\text{O}$ at +13.3 per mil. Samples S-1 and S-3 are from a 5 meter wide quartz vein about 100 meters northwest of the main entrance; S-8 and S-12 are from the quartz vein near the main entrance; and, SP-6 is from the dump and is associated with the mineralization. The calculated $\delta^{18}\text{O}$ value for the hydrothermal fluid is +4.9 per mil, assuming a equilibrium temperature of 275°C (trapping

temperature).

The similarity of oxygen isotopic compositions of different veins throughout the area indicates that the hydrothermal fluids responsible for the deposition of the quartz and mineralization are genetically related to each other.

Five whole rock measurements made on the quartz-schist give the $\delta^{18}\text{O}$ values from +11.7 to +16.7 per mil (table 3). Two samples (FA-13 and FA-17) from Fairview are from within the ore-zone and show some alteration (silicification, carbonitization and sericitization). A small quartz vein (FA-13-V) cuts through the sample FA-13. The other three samples (M-5, M-6 and M-7) from Morning star were collected from outside of the ore-zone, about 150 to 200 meters northeast of the main entrance, and show no alteration. The discrepancy of the $\delta^{18}\text{O}$ for quartz-schist is attributed to two reasons: 1) higher content of the quartz in the rock makes the sample higher ^{18}O value, e.g., sample M-7 composed basically of the quartz has the highest $\delta^{18}\text{O}$ value; 2) oxygen isotopic exchange between rocks and hydrothermal fluids decreases ^{18}O of the rock, e.g., sample FA-13 has the lowest $\delta^{18}\text{O}$ value, due to the direct contact with the quartz vein.

The $\delta^{18}\text{O}$ values of three chlorite-schist samples range from +5.7 to +8.3 per mil. These samples are from 250 to 500 meters east of the Morning Star main shaft.

Several $\delta^{18}\text{O}$ values of separated mineral samples from country rocks have been analysed with the purpose of understanding regional metamorphic setting. Sample M-6-Q and M-7-Q, the quartz separated from quartz-schist samples M-6 and M-7, have their $\delta^{18}\text{O}$ values of +15.1 and +16.6 per mil, respectively, which are 2-3 per mil higher than that of the vein quartz and indicate some difference between them. A biotite sample (M-7-B) gives $\delta^{18}\text{O}$ value of +9.5 per mil. According to O'Neil et al. (1975), quartz-biotite fractionation can be estimated from quartz-muscovite expression by assuming that

$$\Delta_{\text{quartz-muscovite}} = 0.54 \Delta_{\text{quartz-biotite}}$$

for muscovite-containing metamorphic rocks. In sample M-7, the coexisting quartz and biotite have their Δ value of 7.1 per mil. As a consequence, the calculated equilibrium temperature is $431 \pm 30^\circ\text{C}$, using Bottinga et al.'s (1973) quartz-water and muscovite-water fractionation data (see also Friedman et al., 1977, their figure 24). This temperature may represent the metamorphic temperature. Making an approximation of 400°C for metamorphism, the metamorphic fluid should have a $\delta^{18}\text{O}$ value of about +10.4 per mil, using Clayton et al.'s (1972) equation and assuming a $\delta^{18}\text{O}$ value of +15 per mil for metamorphic quartz. This value is 5-6 per mil higher than $\delta^{18}\text{O}$ value of hydrothermal fluid.

Sample M-8-Ch is a chlorite sample separated from the sample M-8 and has the $\delta^{18}\text{O}$ value of +5.1 per mil.

The quartz(M-8-V-Q) and calcite(M-8-V-Ca) separated from quartz-calcite vein(M-8-V), which cuts through M-8, have $\delta^{18}\text{O}$ values of +12.8 and +9.7, respectively. The oxygen isotopic fractionation between quartz and calcite here yields an equilibrium temperature of $308^{\circ}\pm 30^{\circ}\text{C}$, based on Bottinga et al.'s(1973) data for quartz-water system and revised O'Neil et al.'s(1969) data for calcite-water system(see also Friedman et al., 1977, their figure 24). Using the fractionation data of quartz-chlorite(Wenner et al., 1971), the calculated equilibrium temperature is $320^{\circ}\pm 20^{\circ}\text{C}$ for $\Delta_{\text{quartz-chlorite}} = 7.7$ per mil. This temperature is very close to quartz-calcite temperature and indicates that the hydrothermal fluid was isotopically equilibrated with the rocks it passed. This may be the reason why the $\delta^{18}\text{O}$ value of sample M-8(+5.7 per mil) is lower than that of other two chlorite-schist samples(+7.0 and +8.3 per mil), which may more represent the regional metamorphic background.

The oxygen isotopic data show that two kinds of fluids, hydrothermal and metamorphic, existed in this area in geological history. The temporal relationship between these two fluids has not been well established, but judging from that the quartz veins generally follow the regional schistosity, the hydrothermal fluid may be younger than the metamorphic fluid.

6.2.2.2 Carbon isotopic composition

Three CO₂ samples of inclusion fluid, two from Fairview (FA-13-V and FA-24) and one from Morning Star (M-16), have uniform carbon isotopic composition, with the variation of $\delta^{13}\text{C}$ only 0.7 per mil (table 3). This further supports the assumption that the hydrothermal ore-forming fluids have an identical origin in Fairview area.

The $\delta^{13}\text{C}$ values of -8.2--8.9 per mil for CO₂ are a little lighter than that of "juvenile" carbon, which is generally assumed to have the $\delta^{13}\text{C}$ values between -4 and -8 per mil (e.g., Deneis et al., 1973; Ozima et al., 1985), but heavier than that of "normal" graphite and organic compounds, which usually have $\delta^{13}\text{C}$ values between -10 and -35 per mil (Ohmoto et al., 1979). Various authors (e.g., Hoefs et al., 1979; Kreulen, 1980) have suggested three different possibilities for the source of CO₂ in the fluids: 1) decarbonation, 2) oxidation of organic matter, and, 3) juvenile CO₂ or homogenized crustal carbon, i.e., deep-seated origin. Ohmoto et al. (1979) suggested that a hydrolysis reaction of reduced carbon may be the source of the carbon in hydrothermal fluids. Since the lithostratigraphy regionally contains no carbonate rock, the decarbonation origin can be excluded. Juvenile carbon is isotopically heavier than CO₂ from inclusion fluid. Thus, if juvenile carbon is involved in the fluid, a certain amount of light carbon,

most probably carbon from organic matter, is involved. Nevertheless, the most probable CO_2 source is the combination of oxidation and hydrolysis of reduced carbon at higher temperature. The oxidation reaction, $\text{C} + \text{O}_2 \rightarrow \text{CO}_2$, produces CO_2 , which has $\delta^{13}\text{C}$ similar to organic carbon of -10 to -35 per mil, and the hydrolysis reaction, $2\text{C} + 2\text{H}_2\text{O} \rightarrow \text{CO}_2 + \text{CH}_4$, heavier carbon with $\delta^{13}\text{C}$ of 3 to 12 per mil heavier than organic carbon (Ohmoto et al., 1979). The combination of the two can result in a carbon isotopic composition similar to that observed in the Fairview area. The existence of graphite in host rocks and CH_4 in fluids supports this assumption.

A calcite sample (M-8-V-Ca) gives a $\delta^{13}\text{C}$ value of -9.1 per mil. This value is slightly lighter (0.2 to 0.9 per mil) than that of inclusion fluid CO_2 . The calculated fractionation of $\delta^{13}\text{C}$ between CO_2 gas and calcite at 285°C is 1.7 per mil, according to Bottinga's (1968) data, which is close to the result we have obtained from carbon isotopic study. This indicates that the calcite precipitated from the hydrothermal fluid had reached equilibrium with the fluid. This is consistent with the oxygen isotope study. A further inference is that the carbonatization developed near the veins is due to the hydrothermal activity.

6.2.3 Oro Fino Camp

Three quartz samples of Oro Fino deposit have a narrow range of $\delta^{18}\text{O}$ from +11.8 to +12.5 per mil (table 4). Among them, sample O-1 is from a 2 meters thick quartz vein and O-8 a 10 cm thick quartz vein. Both occur near the main shaft. Sample O-11 is from the waste dump and may be associated with the ore.

Three quartz samples from Twin Lake deposit have similar $\delta^{18}\text{O}$ values from +10.8 to +12.7 per mil, although two of them (T-11 and T-12) are from a vein about 100 meters away the main shaft and one (T-10) from a dump and may be associated with the ore.

The similarity of the oxygen isotopic compositions between the quartz from Oro Fino and Twin Lake indicates that both ore-containing and barren quartz veins were originated from the same kind of fluid. Fluid inclusion studies have shown a formation temperature of about 330°C for these quartz samples. Using Clayton et al.'s equation (1972), the calculated $\delta^{18}\text{O}$ values of the water are from +4.4 to +6.3 per mil. These oxygen isotopic constituents are compatible to those from Fairview area, from +3.4 to +6.0, indicating a genetic relationship between them.

Whole rock oxygen isotopic compositions from 5 samples show relatively scattered values (table 4). $\delta^{18}\text{O}$ values of three amphibolite samples (O-6, O-7 and T-4) from near the main shafts of Oro Fino and Twin Lake range from +1.9 to +6.7 per mil. Two gneissic amphibolite (or hornblende gneiss)

TABLE 4. OXYGEN ISOTOPIC COMPOSITIONS OF
QUARTZ AND ROCKS FROM ORO FINO AND TWIN
LAKE

Sample	Mineral/Rock	$\delta^{18}\text{O}$
O-1	Quartz	+11.8
O-8	Quartz	+12.3
O-11	Quartz	+12.5
O-6	Amphibolite	+5.2
O-7	Amphibolite	+6.7
O-18	Gneissic amphibolite	+4.4
T-1	Gneissic amphibolite	+3.4
T-4	Amphibolite	+1.9
T-10	Quartz	+11.8
T-11	Quartz	+10.8
T-12	Quartz	+12.7

samples (O-18 and T-1) have the $\delta^{18}\text{O}$ values of +4.4 and +3.4 per mil, respectively. It should be noticed that the sample O-18 is from the mine dump and is considered to be more or less related to the ore and the sample T-1 is from 300 meters away the main shaft of the Twin Lake deposit. If the sample T-4 ($\delta^{18}\text{O} = +1.9$ per mil) is excluded, the $\delta^{18}\text{O}$ values would be quite close, from +3.4 to +6.7 per mil. These values are much lower than that of schists of Fairview area and also lower than that of common metamorphic rocks. This may be because either a low $\delta^{18}\text{O}$ fluid reacted with the rocks or the rocks originally had an uncommon low $\delta^{18}\text{O}$ value or both.

7. MODEL OF THE MINERALIZATION

A compilation of the characteristics of the hydrothermal fluids for Dusty Mac, Oro Fino and Fairview is presented in table 5. Two distinct fluids can be recognized from the comparison of the characteristics of the fluids (Fig. 23, Fig. 24). At Dusty Mac, the fluid had an extremely low salinity, low $\delta^{18}\text{O}$ values and very low CO_2 contents and the ore was precipitated at a relatively shallow depth. At Oro Fino and Fairview, the fluids were low salinity, but had high $\delta^{18}\text{O}$ values and high CO_2 contents, and the ore was precipitated at a relatively deep depth. Two general terms, epithermal (Dusty Mac), and mesothermal (Oro Fino and Fairview), are used here to describe two kinds of gold mineralization in the Okanagan Valley.

7.1 Epithermal Mineralization

Numerous studies on Tertiary epithermal precious and base metal deposits (e.g., Nash, 1972; O'Neil et al., 1974; Hayba, 1983) have shown that in this type of deposit, the fluid inclusions usually have homogenization temperatures of $200^\circ\text{--}300^\circ\text{C}$, and low salinities. For example, the fluid involved in the formation of the Au-Ag veins of National district in Nevada were dilute, with the salinity of 1-2 wt% NaCl equivalent (Virke, 1985). The salinity of the fluid for Au-Ag and base metal veins of Sunnyside in Colorado were 0.5-1 wt% NaCl equivalent (Casadevall et al., 1977). Isotopic studies show low $\delta^{18}\text{O}$ and δD values for this type of deposit.

TABLE 5. SUMMARY OF THE
CHARACTERISTICS OF HYDROTHERMAL
ORE-FORMING FLUIDS IN THE OKANAGAN VALLEY

	Dusty Mac	Oro Fino	Fairview
Temperature (°C)	≈240	≈330	≈280
Depth (meters)	≥380	≈3600	≈4000
Salinity (wt%NaCl)	≈0.5	≈6	≈4
CO ₂ content	Very low	High	High
δ ¹⁸ O _{H₂O} SMOW (‰)	-7--9	+4--6	+4--6
δ ¹³ C _{CO₂} PDB (‰)			-8--9
W/R ratio	1-2		

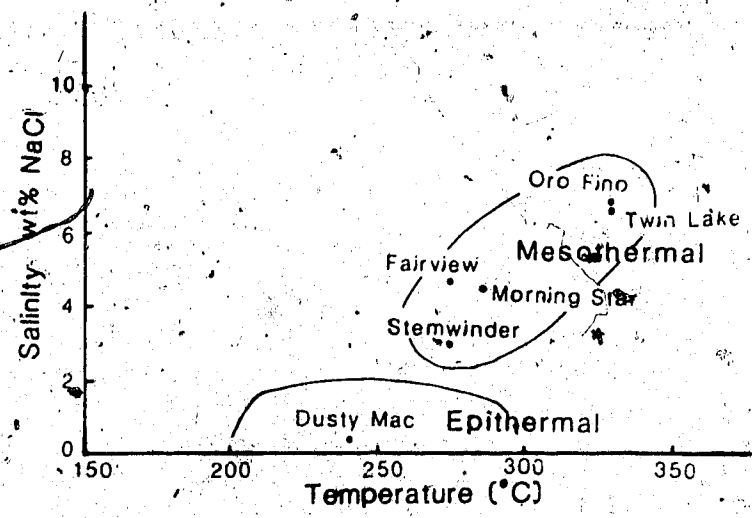


Fig. 23. Temperature-salinity relationship of the hydrothermal ore-forming fluids in the Okanagan Valley.

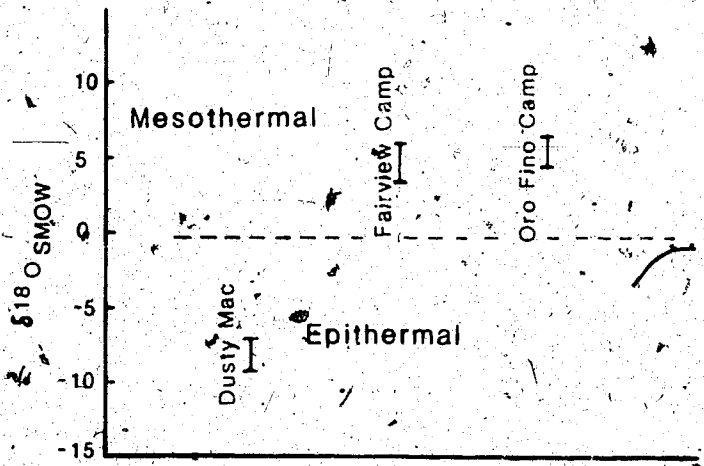


Fig. 24. Oxygen isotopic compositions of the hydrothermal ore-forming fluids in the Okanagan Valley.

For example, O'Neil et al. (1974) studied the isotopic compositions of some epithermal Au-Ag deposits in terrestrial volcanics in Nevada and found that the $\delta^{18}\text{O}$ and δD for the fluid were -6 to -16 and -90 to -140 per mil, respectively.

All the data on fluid inclusions and oxygen isotopes from Dusty Mac are consistent with the characteristics of the Tertiary epithermal Au-Ag vein deposits described by various authors (O'Neil et al., 1974; Taylor, 1974; Hayba, 1983). A mineralization model involving the circulation of meteoric water in the formation of epithermal deposits has been extensively used and can be applied to the Dusty Mac deposit. As demonstrated in the stable isotope chapter, a large amount of meteoric water flowed through the country rocks at Dusty Mac. It is probable that the ore-forming components leached from the rocks were transferred into the water and concentrated in the ore-forming fluid. A rough calculation indicates that only 0.5 ppb Au needs to be removed from the rocks with a volume of 0.5 km^3 to account for the total gold content of the Dusty Mac deposit.

Figure 25 is an idealized cross section, showing the proposed hydrothermal system for Dusty Mac deposit. An intrusive pluton is presumed as the heating source. Meteoric water penetrated the volcanic pile through the fault and plume fracture system, along the topographic lows of the basin. Driven by heat from the pluton, the metal-carrying capacity of the water increased and the metals were leached from the rocks, enriching the water in ore-forming

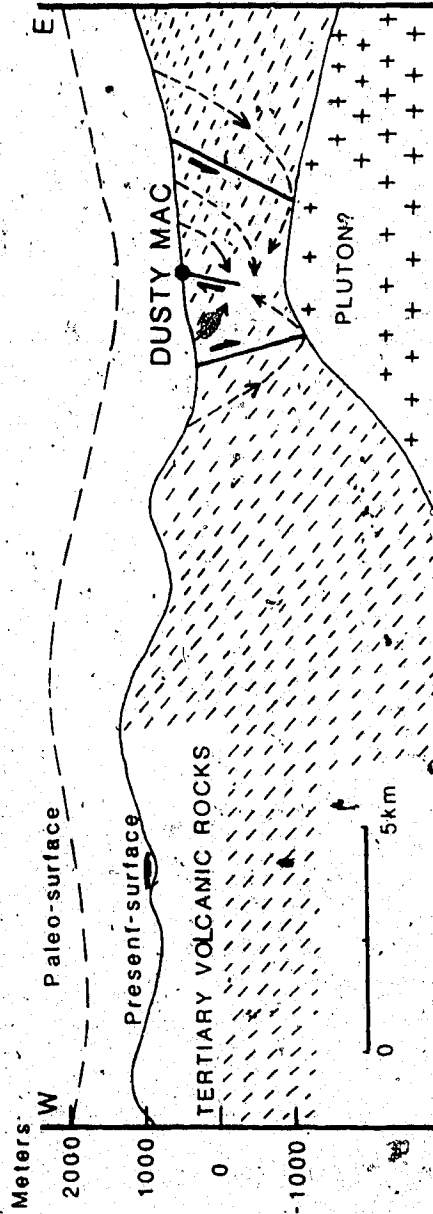


Fig. 25. Idealized cross section showing the proposed hydrothermal system for the formation of the Dusty Mac deposit.

components. Such fluid migrated upward and entered the local fault system, which became the discharge channel. Decreasing temperatures of the fluid acted to decrease the solubilities of the metals and lead to the precipitation of ore minerals. The widespread chloritization and occasional appearance of kaolinite indicate a relatively acid pH environment for mineralization. Such a meteoric model is not new. Many previous studies (e.g., Taylor, 1974, 1979) on the Tertiary Au-Ag deposits in west United States have shown the importance of meteoric water in ore-forming process. The Dusty Mac is a good example in the Canadian Cordillera of this important class of deposits.

7.2 Mesothermal Mineralization

Two generally recognized types of lode gold deposits, the Tertiary epithermal gold deposit and the Archean lode gold deposits, have been extensively studied. The involvement of the meteoric water in Tertiary epithermal gold mineralization (Taylor, 1974, 1979; O'Neil et al., 1974), as discussed above, have been well established. As for Archean lode gold mineralization, most authors hold the point of view that the hydrothermal fluids responsible for mineralizations came from metamorphic dehydration (e.g., Kerrich, 1983; Fyfe and Kerrich, 1984; Grove et al., 1984).

Kerrich and Fyfe (1981) studied Archean greenstone lode gold deposits in Yellowknife, Northwest Territory, and concluded that the CO₂-rich, high $\delta^{18}\text{O}$ ($\delta^{18}\text{O} = +8\text{--}+9$ per mil)

ore-forming fluid was metamorphic in origin and they ascribed the origin of the CO_2 to decarbonation of the carbonate wall rocks. Work by Kerrich and his colleagues (Kerrich and Hodder, 1982; Kerrich, 1983; Kerrich and Watson, 1984; Fyfe and Kerrich, 1984) on Archean greenstone lode gold deposits in Superior Province have shown that the hydrothermal fluids responsible for gold mineralization had a temperature of $320^\circ\text{--}480^\circ\text{C}$, $\delta^{18}\text{O}$ values of $+8\text{--}+11$ per mil and δD values of $-50\text{--}+5$ per mil, with high CO_2 contents and low salinities (less than 2 wt% NaCl equivalent). The authors considered the fluids to be the products of dehydration during metamorphism. Various workers on Archean greenstone lode gold deposits in western Australia (Suzahue et al., 1983; Phillips et al., 1983, 1984; Groves et al., 1984) have shown similar properties ($T = 300^\circ \pm 50^\circ\text{C}$, $\delta^{18}\text{O} = +4.5 \pm 2$ per mil, CO_2 -rich and low salinity) for hydrothermal fluids and the authors also ascribe a metamorphic origin to them.

Some lode gold deposits occurring in Paleozoic or Mesozoic metamorphic rocks show similar characteristics to the Archean lode gold. Graves et al. (1982) reported a CO_2 -rich, low salinity fluid of metamorphic origin for the gold veins in greenschist facies rocks in Nova Scotia. The famous Mother Lode system of California is a series of vein gold deposits occurring in low to intermediate grade metamorphic rocks. Various works (Radtke et al., 1980; Marshall et al., 1980; Raymond, 1981; Weir et al., 1984; Bohlke et al., 1986) have shown that the fluids were

CO₂-rich, with $\delta^{18}\text{O} = +8\text{--}+16$, $\delta\text{D} = -50\text{--}-80$ and $\delta^{13}\text{C} = -2\text{--}-4$ per mil. The authors also considered the fluids to have been derived from metamorphism, but Mashall et al. (1980) showed that the fluid contained mantle-derived CO₂ and some meteoric water, in addition to metamorphic water and CO₂.

However, some Mother Lode type deposits in Canadian Cordillera show lower ^{18}O ($\delta^{18}\text{O} = +2\text{--}+3$ per mil) and D ($\delta\text{D} = -80\text{--}-100$ per mil) values for the fluids (Nesbitt et al., in press) than Mother Lode deposits. Nesbitt et al. (in press) argue that deep circulation of the meteoric water was responsible for the formation of this type of deposits, not the metamorphic fluid, and they suggest that the fluids for Archean lode gold may be the same pattern.

The present study on Fairview and Oro Fino show that these deposits are similar in many aspects to the Archean and Mother Lode gold deposits. Oxygen isotope data indicate that variations of the $\delta^{18}\text{O}$ values for hydrothermal fluids at Fairview and Oro Fino are from +3.4 to +6.3 per mil, with most of the values around +5 per mil. This number is at the lower limit of the metamorphic fluid (Taylor, 1974, 1979) and may give rise to argument for its origin. We have demonstrated that the metamorphic fluid is isotopically different from the hydrothermal fluid in this area, thus two fluids should originate from different sources. Isotopic exchange between country rocks and other waters (sea water or meteoric water) may result in a $\delta^{18}\text{O}$ value of +5 per mil for the hydrothermal fluid. For example, consider a meteoric

water having a $\delta^{18}\text{O}$ value of -13 per mil in contact with a schist having a $\delta^{18}\text{O}$ value of +15 per mil. The calculated $\delta^{18}\text{O}$ value for the fluid could vary between the original -13 and +4.5 per mil, at the water-rock ratio (W/R)=0.2 and temperature of 300°C depending on the degree of isotopic equilibration between the two. Since all geological data indicate that the mineralization occurred in a terrestrial environment, sea water seems unimportant. The most possible source of the hydrothermal fluid is meteoric water. As indicated by the fluid inclusion studies, the fluids ascended from at least 3-4 km below the surface at a relatively high temperature. Assuming a meteoric origin, the water could effectively exchange its isotopic composition with the rocks it passed through and gain a higher $\delta^{18}\text{O}$ value. Nesbitt et al. (in press) have pointed out that the meteoric model can best explain the large amounts of fluid involved in ore formation process. If all the vein quartz was precipitated from the hydrothermal fluid, a simple calculation can give an estimate of the volume of the water involved. At Fairview deposit, the main ore-containing vein has the dimension of at least $200 \times 200 \times 5 \text{ m}^3$ (strike \times dip \times thickness). The solubility of SiO_2 in water is a function of temperature and pressure (Kennedy, 1950; and others, see Holland et al., 1979). Calculation shows that the required water for formation of such quartz vein should be 0.6×10^9 tonnes (0.6 km^3 water) as the temperature of the fluid decrease from 400°C to 300°C, assuming the solubility of the SiO_2 in water

is 0.18 wt% at 400°C and 1 kb and 0.09 wt% at 300°C and 1 kb (Kennedy, 1950) and a specific gravity of 2.5 for quartz. It is interesting that this number is comparable with that we have obtained from oxygen isotope study for Dusty Mac. Considering that many quartz veins exist in this area, the volume of water involved in their deposition must be considerably larger than the volume calculated here. Since the mineralization happened at a deep level (3-4 km), the water must be active at even deeper level. The extensional fault system (Tempelman-Kluit et al., 1986) in Okanagan area could be excellent channel(s) for descending meteoric water. Figure 26A shows an idealized mineralization section. The meteoric water penetrated the rocks at relatively shallow level and descended downward following the normal fault(s), then moved along the gentle dipping detachment zone (Tempelman-Kluit et al., 1986) towards the west. The heated and mineralized water then ascended along the tensional faults and deposited the ore at favourable locations. Assuming the detachment zone extends 20 km horizontally, with the dipping angle of 15°, at the west end, the vertical distance between the detachment and the surface should be 5-6 km. The estimate that the mineralization of Fairview and Oro Fino occurred at a depth of 3-4 km seems to fit this model. A question remains as to the source of heat. If the water was heated by normal thermal gradient (30°C/km), at 5-6 km depth, temperature would be 150-180°C, which is much lower than the temperature from fluid inclusion studies.

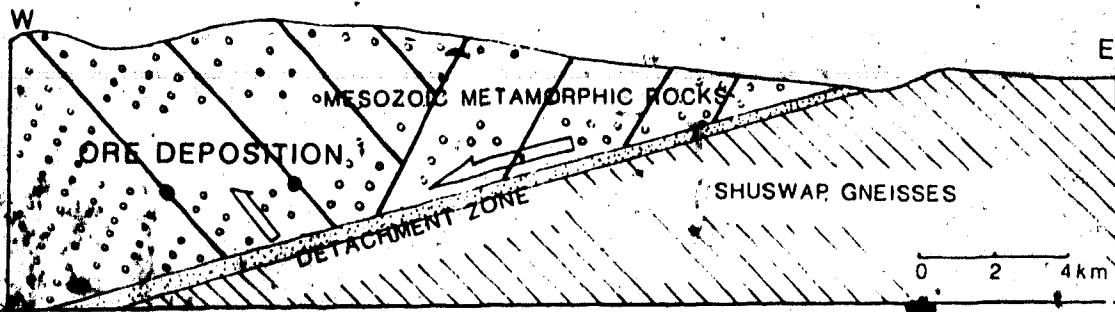


Fig. 26A. Idealized cross section showing the detachment zone and extensional fault system as channel for deep circulation of meteoric water. The ore deposited when the fluids ascend along the detachment zone.

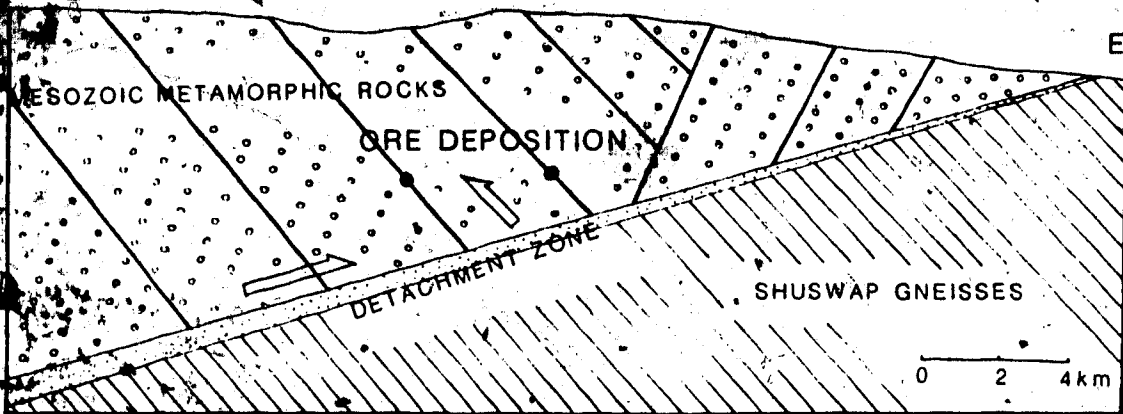


Fig. 26B. Cross section showing the fluids flowing along the detachment zone from west to east.

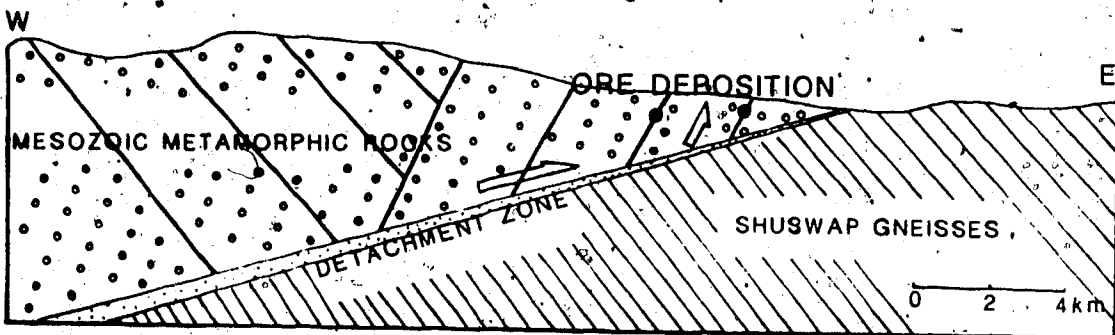


Fig. 26C. Tempelman-Kluit's (1984) mineralization model.

Nevertheless, various authors (Ross, 1974; Medford, 1975; Mathews, 1981) have described a thermal event in Okanagan area in Eocene. Mathews (1981) estimated that the thermal gradient was $37-100^{\circ}\text{C}/\text{km}$ at the time. If this is valid, the water would be sufficiently hot at the required depth. However, it is critical for this model that hydrothermal activity (or mineralization) should have an age of Tertiary to coincide with the fault system and the thermal event.

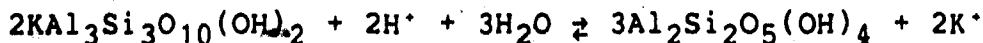
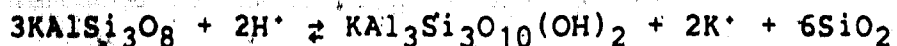
Unfortunately, age-dating for mineralization has not been available at the time of writing. Even though, we believe the effectiveness of the model, since it is consistent with the data obtained from fluid inclusion and stable isotope work.

In this model, the fluids flowed from east to west along the detachment zone. Another possibility of deep circulation of meteoric water is that the fluids flowed from west to east (Fig. 26B). This needs even deeper penetration of the water and the effectiveness of this model is hard to evaluate, because no data are available to show such deep fault systems existing to the west of the Okanagan Valley and whether the water can descend to such a depth is questionable.

In Tempelman-Kluit's (1984) model (Fig. 26C), the ore was deposited at a shallow level, which is inconsistent with the observations in this study.

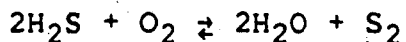
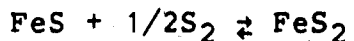
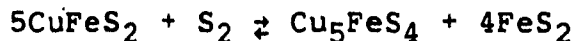
Data for other physicochemical parameters, such as pH, Eh, are not as easily determined, however, some estimates can be made from the mineral assemblages.

Limits on the pH of the fluid can be determined using the following reactions:



At Fairview and Morning Star deposits, sericite occurs as an alteration mineral, neither K-feldspar nor kaolinite has been found as a vein-related mineral. Assuming the activity of the K^+ (a_{K^+}) of the fluid was 10^{-2} (assuming the salinity of the fluid is 4 wt% NaCl, $\text{K}^+/\text{Na}^+ = 0.1$, and $I = 0.25$, the a_{K^+} can be estimated as 0.01 mol/kg H_2O), at 300°C , the stability of the sericite sets the pH range from 5.9 (Fig. 27), compared with the neutral pH of 5.7 at 300° . Change of the a_{K^+} by 10 times may result in the shift of pH by one unit.

The following reactions:



can be used for calculation of the limits on f_{O_2} of the fluid. Mineralogical studies show that pyrite is abundant and pyrrhotite is rare in the ore assemblage, thus pyrite-pyrrhotite line can be used as lower limit for f_{O_2} of the fluid. At the same time, bornite+pyrite - chalcopyrite line can be used as upper limit for f_{O_2} of the fluid, due to the fact that chalcopyrite is a ubiquitous mineral, but bornite just occasionally appears. Calculations show that $\log f_{\text{O}_2}$ limits for above mineral pairs are between -36.2 and -31.0 ($\Sigma S = 0.05\text{m}$) or between -32.8 and -27.6 ($\Sigma S = 0.00\text{fm}$). The

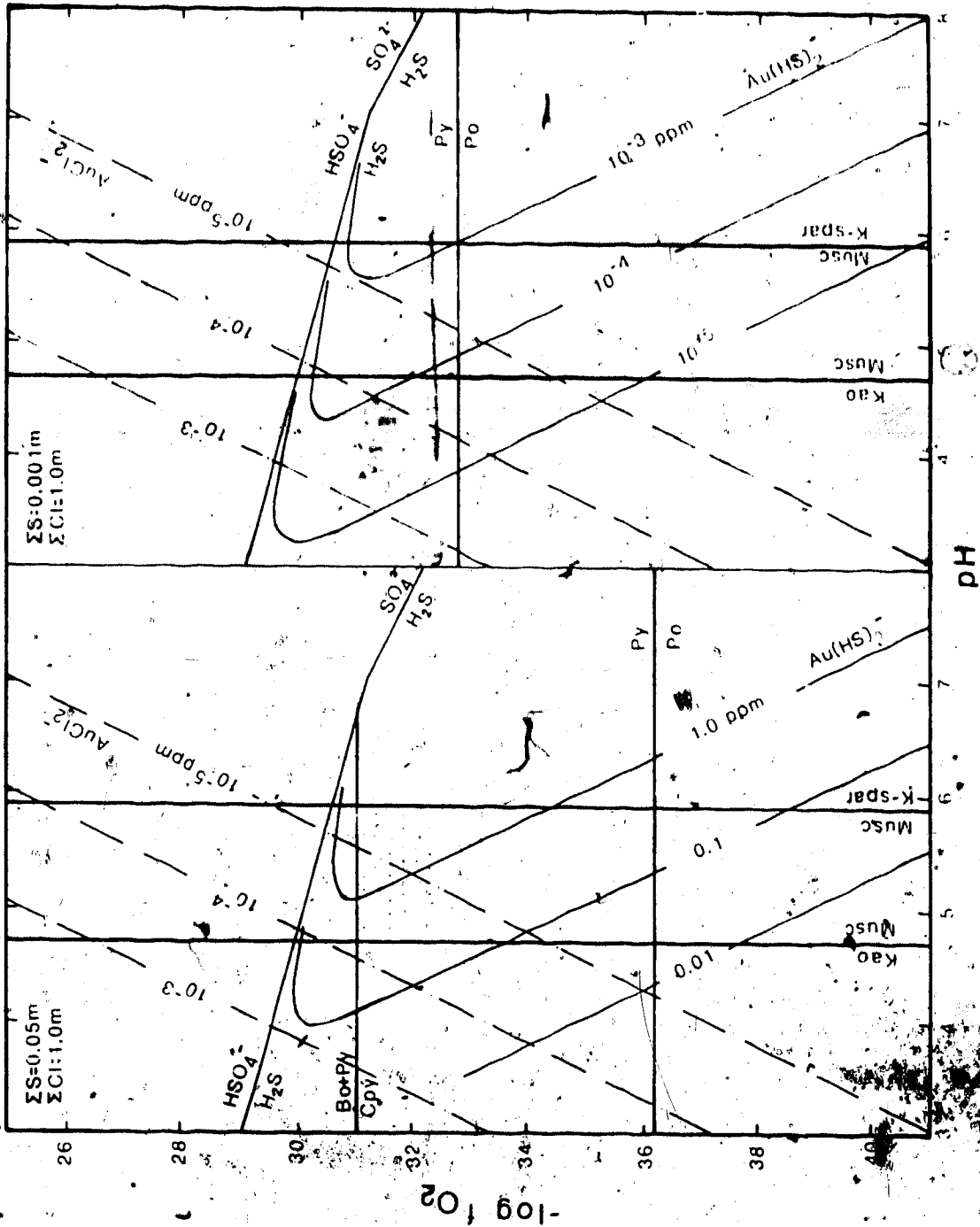


Fig. Gold solubility contours for $Au(HS)_2$ and $AuCl_2^-$ (in ppm) at 300°C. After Helgeson (1969). Thermodynamic data for calculating reactions of kaolinite (Kao), muscovite (Musc), muscovite-K-felspar (K-spar), pyrite (Py), pyrrhotite (Po), bornite (Bo) + pyrite-chalcocopyrite (Cpy), HSO_4^- , H_2S and SO_4^{2-} are from Helgeson (1969). The dotted area indicates the most probable region of deposition.

log f_{O_2} value of -27.6 is higher than the stability limit for reduced sulfur and hence the reaction cannot occur.

The lack of sulfate in the ore assemblages indicates that sulfur species in fluids was reduced sulfur. Therefore, the equilibrium curves between sulfate and sulphide species can be used as a limit of the f_{O_2} . Figure 27 shows that log f_{O_2} limits for H_2S are -29.3 (pH=3) -- -32.3 (pH=8) at 300°C. These limits, together with bornite+pyrite - chalcopyrite line, form the upper limit of f_{O_2} for the fluids.

According to above considerations, the dotted area in Figure 27 is referred to be the preferred region for ore deposition.

In fluid inclusion studies, we have demonstrated that the fluids were effervescing when the vein material precipitated in Fairview area. As a consequence, loss of CO_2 from the fluid could increase the pH. As shown in figure 27, increase pH by one unit, the solubility of $AuCl_2^-$ decreases 80-90%. At the same time, the solubility of $Au(HS)_2^-$ increases approximately by the same amount. At the pH range of 4.7-5.9 and log f_{O_2} of -27 -- -37, the dominant gold species may be either $AuCl_2^-$ or $Au(HS)_2^-$ or both (Fig. 27), depending on the activities of Cl^- and the total reduced sulfur. Thus, effervescence of CO_2 may or may not be an important factor in precipitation of the gold. However, the facts that the fluid shows no effervescence in Oro Fino and the mineralization happened over a considerable vertical distance indicate that other factors are probably in controlling the precipitation

of the gold. For example, temperature is a very important controlling factor. According to Seward (1984), temperature decrease from 350°C to 300°C (the situation which is similar to that of Fairview and Oro Fino), the solubilities of both $\text{Au}(\text{HS})_2^-$ and AuCl_2^- decrease by 80-90%. As shown in Figure 27, the solubility of $\text{Au}(\text{HS})_2^-$ drastically decreases (about 2 orders of magnitude), as the total reduced sulfur decreases from 0.05m to 0.001m. This may imply that decrease of total reduced sulfur is another important factor in controlling the gold deposition. The mechanism of decreasing total reduced sulfur can be related to the precipitation of sulphides. This can well explain why the gold usually relates to late stage sulphides (galena and sphalerite), not pyrite of early stage (see mineralization chapter). The fact that the salinity of the fluids were low indicates that the total chloride in fluids was very low. Consequently, the most probable dominant gold species is $\text{Au}(\text{HS})_2^-$ and the main controlling factors in precipitation of the gold may be the decrease of temperature of the fluids due to their upward moving and the decrease of the total reduced sulfur due to the precipitation of sulphides.

8. CONCLUSIONS AND FUTURE WORK

The gold deposits in Okanagan valley can be divided into two groups: epithermal deposits represented by Dusty Mac and mesothermal deposits represented by Fairview and Oro Fino. Two distinct mineralization mechanisms, shallow circulation and deep circulation of the meteoric water, were responsible for the formation of the two groups of gold deposits. A detailed study of fluid inclusions and stable isotopic compositions of the minerals and rocks has shown that the above assumptions are valid. Nevertheless, in spite of these conclusions, some problems still exist:

(1). The temporal relationship between hydrothermal mineralization and metamorphism has not been well established. Most of the data obtained from the studies of the fluid inclusions and stable isotopes can be explained either by deep circulation of the meteoric water or ascending of the metamorphic water or the mixing of the two. The oxygen isotope study has demonstrated the isotopic difference between these two fluids. If we can prove a difference in ages (presumably a Jurassic age for metamorphism and a Tertiary age for mineralization), the distinction between the two events would be more apparent.

(2). The lack of hydrogen isotope data complicates the testing of the meteoric water theory. It is believed that the δD values of the fluids will be fairly low to fit the meteoric $\delta^{18}O$ - δD relationship. However, the analytical results for δD have not been obtained to date.

(3). The estimation of the depth of mineralization is still questionable. As discussed before, for H_2O-CO_2-NaCl system; at the temperatures of interest ($200^{\circ}-350^{\circ}C$), slight changes of the temperature and salinity can drastically shift the immiscibility curve. This would influence the pressure estimate. Since all the temperature and salinity data were from statistics of the fluid inclusion study, errors are inevitable - this may create problems in pressure estimation. Unfortunately, at the state of art, this problem still cannot be solved satisfactorily.

REFERENCE

- Bohlke, J.R. and R.W. Kistler, 1986, Rb-Sr, K-Ar, and stable isotope evidence for the ages and sources of fluid components of gold-bearing quartz veins in the Northern Sierra Nevada Foothills metamorphic belt, California: *Econ. Geol.*, v.81, p.296-322.
- Bostock, H.S., 1941, Okanagan Falls, B.C., Geological map with marginal notes, GSC Map 627A.
- Bottinga, Y., 1968, Calculation of fractionation factor for carbon and oxygen exchange in the system calcite-carbon dioxide-water: *Jour. Phys. Chemistry*, v.72, p.800-808.
- Bottinga, Y., and M. Javoy, 1973, Comments on oxygen isotope geothermometry: *Earth Planet. Sci. Letters*, v.20, p.250-265.
- Bower, T.S., and H.C. Helgeson, 1983a, Calculation of the thermodynamic and geochemical consequence of nonideal mixing in the system H_2O-CO_2-NaCl on phase relations in geologic systems: equation of state for H_2O-CO_2-NaCl fluids at high pressures and temperatures: *Geochim. et Cosmochim. Acta*, v.47, p.1247-1275.
- Bower, T.S., and H.C. Helgeson, 1983b, Calculation of the thermodynamic and geochemical consequence of nonideal mixing in the system H_2O-CO_2-NaCl on phase relations in geologic systems: metamorphic equilibria at high pressures and temperatures: *Am. Mineralogist*, v.68, p.1059-1075.
- Bozzo, A.T., J.R. Chen, and A.J. Barduhn, 1973, The properties of hydrates of chloride and carbon dioxide, in: *Fourth international symposium on fresh water from the sea*, Delyannis, A., and E. Delyannis eds., v.3, p.437-475.
- Burrus, R.C., 1981a, Analysis of phase equilibria in C-O-H-S fluid inclusions, in: *Short course in fluid inclusions*, Mineral. Assn. Can. Short course 6,

- Hollister, L.S., and M.L. Crawford eds., p.39-74.
- Burrus, R.C., 1981b, Analysis of fluid inclusions: phase equilibria at constant volume: *Am. Jour. Sci.*, v.281, p.1104-1126.
- Cairnes, C.E., 1940, Kettle river (West half) B.C., Geological map with marginal notes, GSC Map 538A.
- Casadevall, T., and H. Ohmoto, 1977, Sunnyside mine, Eureka mining district, San Juan County: Geochemistry of gold and base metal ore deposition in a volcanic environment: *Econ. Geol.*, v.72, p.1285-1320.
- Church, N.B., 1969, Dusty Mac, in: B.C. Dept. of Mines and Petroleum Resources, GEM 1969, p.294-295.
- Church, N.B., 1970, White Lake, in: B.C. Dept. of Mines and Petroleum Resources, GEM 1970, p.396-406.
- Church, N.B., 1973, Geology of the White Lake basin: B.C. Dept. of Mines and Petroleum Resources Bull., v.61, 120p.
- Clayton, R.N., and T.K. Mayeda, 1963, The use of bromine pentafluoride in the extraction oxygen from oxides and silicates for isotopic analysis: *Geochim. et Cosmochim. Acta*, v.27, p.43-52.
- Clayton, R.N., J.R. O'Neil, and T.K. Mayeda, 1972, Oxygen isotope exchange between quartz and water: *Jour. Geophys. Research*, v.77, p.3057-3067.
- Cockfield, W.E., 1939, Lode-gold deposits of Fairview Camp, Camp McKinney and Videtle area, and the Divident Lakeview property near Osoyoos, B.C.: GSC Mem., v.179, 38p.
- Collins, P.L.F., 1979, Gas hydrates in CO₂-bearing fluid inclusions and the use of freezing data for estimation of salinity: *Econ. Geol.*, v.74, p.1435-1446.

Craig, H., 1957, Isotopic standards for carbon and oxygen and correction factors for mass spectrometric analysis of carbon dioxide: *Geochim. et Cosmochim. Acta*, v.12, p.133-149.

Craig, H., 1961, Standard for reporting concentrations of deuterium and oxygen-18 in natural waters: *Science*, v.133, p.1833-1834.

Deneis, P., and D.P. Gold, 1973, The isotopic composition of carbonatite and kimberlite carbonates and their bearing on the isotopic composition of deep-seated carbon: *Geochim. et Cosmochim. Acta*, v.37, p.1709-1733.

Ellis, A.J., and R.M. Golding, 1963, The solubility of carbon dioxide above 100°C in water and in sodium chloride solutions: *Am. Jour. Sci.*, v.261, p.47-60.

Friedman, I., and J.R. O'Neil, 1977, Compilation of stable isotope fractionation factors of geochemical interest: USGS Paper, 440-KK, 49p.

Fyfe, W.S., and R. Kerrich, 1984, Gold: natural concentration processes, in: *Gold'82: geology, geochemistry and genesis of gold deposits*, Forster, R.P., ed., p.99-128.

Gabrielse, H., and C.J. Yorath, 1982, The Cordilleran Orogen: Canadian sector, in: *Regional geological synthesis: planning for the geology of North America: D-NAG special publication 1*, Palmer, A.R., ed., p.81-89.

Gehrig, M., H. Lentz, and E.U. Frank, 1979, Thermodynamic properties of water-carbon dioxide-sodium chloride mixtures at high temperatures and pressures, in: *High-pressure science and technology, Sixth AIRAPT conference v.1: Physical properties and material synthesis*, Timmerhaus, K.D., and M.S. Barber eds., p.539-542.

Graves, M. C., and M. Zentilli, 1982, A review of the geology of gold in Nova Scotia, in: *Geology of Canadian gold deposits*, Hodder, R.W., and P. William eds., CIM special volume 24, p.233-242.

- Groves, D.I., G.N. Phillips, S.E. Ho, C.A. Henderson, M.E. Clark, and G.M. Woad, 1984, Controls on distribution of Archean hydrothermal gold deposits in western Australia, in: Gold'82: geology, geochemistry and genesis of gold deposits, Foster, R.P. ed, p.689-712.
- Hass, J.L. Jr, 1971, The effect of salinity on the maximum thermal gradient of a hydrothermal system at hydrostatic pressure: Econ. Geol., v.66, p.940-946.
- Hass, J.L. Jr, 1976, Physical properties of the coexisting phases and thermochemical properties of the H₂O component in boiling NaCl solutions: USGS Bull., 1421-A, 73p.
- Hayba, D.O., 1983, A compilation of fluid inclusion and stable isotope data on selected precious- and base-metal epithermal deposits: USGS Open-file report, 83-450, 24p.
- He, Zhili, 1980, Inclusion mineralogy, 280p. (in Chinese)
- Hedley, M.S., and K.D. Watson, 1945, lode-gold deposits, central southern British Columbia: B.C. Dept. of Mines Bull., No. 20, Part 3, 27p.
- Helgeson, H.C., 1969, Thermodynamics of hydrothermal systems at elevated temperatures and pressures: Am. Jour. Sci., v.267, p.729-804.
- Hoefs, J., and G. Morteani, 1979, The carbon isotopic composition of fluid inclusions in Alpine fissure quartzes from the western Tauern Window (Tyrol, Austria): Neues Jahrb. Mineral. Monatsh, 1979 No.3, p.123-134.
- Holland, H.D. and S.D. Malinin, 1979, The solubility and occurrence of non-ore minerals, in: Geochemistry of hydrothermal ore deposits, Barnes, H.L., ed, John Wiley and Sons, p.461-508.
- Hollister, L.S., and R.C. Burrus, 1976, Phase equilibria in fluid inclusions from the Khtada Lake metamorphic complex: Geochim. et Cosmochim. Acta, v.40,

p.163-175.

Kamilli, R.J., and H. Ohmoto, 1977, Paragenesis, zoning, fluid inclusion and isotopic studies of the Finlandia vein, Colqui District, Central Peru: Econ. Geol., v.72, p.950-982.

Kennedy, G.C., 1950, A portion of the system of silica-water: Econ. Geol., v.45, p.629-653.

Kennedy, G.C., 1954, Pressure-volume-temperature relations in CO₂ at elevated temperatures and pressures: Am. Jour. Sci., v.252, p.225-241.

Kerrick, R., 1983, Geochemistry of gold deposits in the Abitibi greenstone belt: CIM special volume 27, 75p.

Kerrick R., and W.S. Fyfe, 1981, The gold-carbonate association: source of CO₂, and CO₂ fixation reactions in Archean lode deposits: Chemical Geology, v.33, p. 265-294.

Kerrick, R., and R.W. Hodder, 1982, Archean lode gold and base metal deposits: evidence for metal separation into independent hydrothermal systems, in: Geology of Canadian gold deposit, Hodder R.W., and P. William eds., CIM special volume 24, p.144-160.

Kerrick, R., and G.P. Watson, 1984, The Macassa mine Archean lode gold deposit, Kirtland Lake, Ontario: Geology, Patterns of alteration, and hydrothermal regimes: Econ. Geol. v. 79, p.1104-1130.

Kreulen, R., 1980, CO₂-rich fluids during regional metamorphism on Naxos(Greece): carbon isotopes and fluid inclusions: Am. Jour. Sci., v.280, p.745-771.

Little, H.W., 1961, Geology, Kettle river(West half), British Columbia; GSC Map 15, 1961.

Magaritz, M., and H.P. Taylor Jr, 1986, Oxygen 18/Oxygen 16 and D/H studies of plutonic granitic and metamorphic rocks across the Cordilleran batholiths of southern

British Columbia: Jour. Geophy. Research, v.91,
p.2193-2217.

Marshall, B., and B.E. Taylor, 1980, Origin of hydrothermal fluids responsible for gold deposition, Alleghany District, Sierra County, California: GSA abstracts with programs, v.12, p.118.

Mathews, W.H., 1964, Potassium-Argon age determinations of Cenozoic volcanic rocks from British Columbia at GSA Bull., v.75, p.465-468.

Mathews, W.H., 1981, Early Cenozoic resetting of potassium-argon dates and geothermal history of north Okanagan area, British Columbia: Can. Jour. Earth Sci., v.18, p.1316-1319.

McCrea, J.M., 1950, On the isotopic chemistry of carbonates and a paleotemperature scale: Jour. Chem. Physics, v.18, p.849-857.

Medford, G.A., 1975, K-Ar and fission track geochronometry of an Eocene thermal event in the Kettle river (West half) map area, southern British Columbia: Can. Jour. Earth Sci., v.12, p.836-843.

Minister of Mines, B.C., 1933, Annual report, Southern and central district (Nos. 3 and 4), p.146-198.

Minister of Mines and Petroleum Resources, B.C., 1975, Annual Report, Chapter 3, Mineral resource statistics, p.A51-A97.

Minister of Mines and Petroleum Resources, B.C., 1976, Annual Report, Chapter 3, Mineral resource statistics, p.A61-A106.

Monger, J.W.H., and R.A. Price, 1979, Geodynamic evolution of the Canadian Cordillera - progress and problems: Can. Jour. Earth Sci., v.16, p.770-792.

Monger, J.W.H., R.A. Price, and D.J. Tempelman-Kluit, 1982, Tectonic accretion and the origin of the two major

metamorphic and plutonic belts in the Canadian Cordillera: *Geology*, v.10, p.70-75.

Nash, J.T., 1972, Fluid inclusion studies of some gold deposits in Nevada: USGS Prof. Paper, 800-C, p.c-15-c-19.

Nesbitt, B.E., J.B. Murowchick, and K. Muehlenbachs, Dual origins of lode gold deposits in the Canadian Cordillera. (in press)

Ohmoto, H., and R.O. Rye, 1979, Isotopes of sulfur and carbon, in: *Geochemistry of hydrothermal ore deposits*, 2nd edition, Barnes H.L. ed., John Wiley and Sons, p.509-567.

Okulitch, A.V., 1983, The role of Shuswap metamorphic complex in Cordillerian tectonism: a review: *Can. Jour. Earth Sci.*, v.21, p.1171-1193.

O'Neil, J.R., and H.P. Taylor Jr, 1967, The oxygen isotopic and cation exchange chemistry of feldspar: *Am. Mineralogist*, v.52, p.1414-1437.

O'Neil, J.R., R.N. Clayton, and T.K. Mayeda, 1969, Oxygen isotope fractionation in divalent metal carbonates: *Jour. Chem. Physics*, v.51, p.5547-5558.

O'Neil, J.R., and M.L. Silberman, 1974, Stable isotope relations in epithermal Au-Ag deposits: *Econ. Geol.*, v.69, p.902-909.

O'Neil, J.R., and E.D. Ghent, 1975, Stable isotope study of coexisting metamorphic minerals from the Esplanade Range, British Columbia: *GSA Bull.*, v.86, p.1708-1712.

Ozima, M., S. Zashu, D.P. Matthey, and C.T. Pillinger, 1985, Helium, argon and carbon isotopic compositions in diamond and their implications in mantle evolution, *Geochemical Jour.*, v.19, p.127-134.

Parrish, R., S. Carr, and Parkison, 1985, *Metamorphic*

- complexes and extensional tectonics, southern Shuswap complex, Southeastern British Columbia, in: Field guides to geology and mineral deposits in the southern Canadian Cordillera, GSA Cordilleran section meeting, Vancouver, B.C., May '85, ed. by Tempelman-Kluit, D., p.12-1-12-15.
- Peto, P., 1973, Petrochemical study of the Similkameen batholith, British Columbia: GSA Bull., v.84, p.3977-3984.
- Peto, P., and R.C. Armstrong, 1976, Strontium isotope study of the composite batholiths between Princeton and Okanagan Lake: Can. Jour. Earth Sci., v.13, p.1577-1583.
- Phillips, G.N., and D.I. Groves, 1983, The nature of Archean gold fluids as deduced from gold deposits in western Australia: Geol. Soc. Australia Jour., v.30, p.25-39.
- Phillips, G.N., and D.I. Groves, 1984, Fluid access and fluid-wallrock interaction in the genesis of Archean Gold-quartz vein deposit at Hunt mine, Kambalda, Western Australia, in: Gold'82: geology, geochemistry and genesis of gold deposits, Forster, R.P. ed., p.389-418.
- Potter, R.W., 1977, Pressure corrections for fluid-inclusion homogenization temperatures based on the volumetric properties of the system NaCl-H₂O: USGS Jour. Res., v.5, p.603-607.
- Potter, R.W., M.A. Clyne, and D.L. Brown, 1978, Freezing point depression of aqueous sodium chloride solutions: Econ. Geol., v.73, p.284-285.
- Price, R.A., J.W.H. Monger, and J.A. Roddick, 1985, Cordilleran cross section: Calgary to Victoria, in: Field guides to geological and mineral deposits in the southern Canadian Cordillera, Tempelman-Kluit, D., ed., p.3-1-3-85.
- Radtke, A.S., W.H. Wittkopp, and C. Heropoulos, 1980, Genesis of gold-bearing quartz veins of the Alleghany District, Calif.: GSA abstracts with programs, v.12

p. 148.

- Raymond, M.C. Jr, 1981, Gold quartz veins and auriferous granite at Oriental mine, Alleghany District, California: Econ. Geol., v.76, p.2176-2199.
- Robie, R.A., B.S. Hemingway, and J.R. Fisher, 1978, Thermodynamic properties of minerals and related substances at 298.15K and 1 bar (10^5 pascal) pressure and at higher temperatures: USGS Bull., v.1452, 456p.
- Roedder, E., 1963, Studies of fluid inclusions 2: freezing data and their interpretation: Econ. Geol., v.58, p.167-221.
- Roedder, E., 1979, Fluid inclusions as samples of ore fluids, in: Geochemistry of hydrothermal ore deposits, 2nd edition, Barnes, H.L. ed., John Wiley and Sons, p.684-731.
- Roedder, E., 1984, Fluid inclusions, Reviews in mineralogy V. 12; Mineral. Society of America, 644p.
- Roedder, E., and R.J. Bodnar, 1980, Geologic pressure determinations from fluid inclusion studies: Annu. Review Earth Planet. Sci., v.8, p.263-301.
- Ross, J.V., 1974, A Tertiary thermal event in south-central British Columbia: Can. Jour. Earth Sci., v.11, p.1116-1122.
- Ross, J.V., and J.S. Christie, 1979, Early recumbent folding in some westmost exposures of the shuswap complex, southern Okanagan, British Columbia: Can. jour. Earth Sci., v.16, p.877-894.
- Seward, T.M., 1984, The transport and deposition of gold in hydrothermal systems, in: Gold'82: the geology, geochemistry and genesis of gold deposits, Foster, R.P., ed., p.165-181.
- Sugisaki, R., and M.L. Jensen, 1971, Oxygen isotopic studies of silicate minerals with special reference to

- hydrothermal mineral deposits: *Geochem. Jour.*, v.5, p.7-21.
- Suzahue, D.G., and A.F. Wilson, 1983, Geochemical and stable isotopes of the No. 4 lode, Kalgoorlie, western Australia: *Econ. Geol.*, v.78, p.438-450.
- Swanenberg, H.E.C., 1979, Phase equilibria in carbonic systems and their application to freezing studies of fluid inclusions: *Contrib. Mineral. Petrol.*, v.68, p.303-306.
- Takenouchi, S., and G.C. Kennedy, 1965, The solubility of carbon dioxide in NaCl solutions at high temperatures and pressures: *Am. Jour. Sci.*, v.263, p.445-454.
- Taylor, H.P. Jr, 1974, The application of oxygen and hydrogen isotope studies to problems of hydrothermal alteration and ore deposition: *Econ. Geol.*, v.69, p.843-883.
- Taylor, H.P. Jr, 1977, Water/rock interaction and the origin of H₂O in granitic batholiths: *Geol. Soc. Lond.*, v.133, p.360-393.
- Taylor, H.P. Jr, 1979, Oxygen and hydrogen isotope relations in hydrothermal mineral deposits, in: *Geochemistry of hydrothermal ore deposits*, 2nd edition, Barnes H.B. ed., John Wiley and Sons, p.236-277.
- Taylor, M., S.F. Kesler, P.L. Cloke, and W.C. Kelly, 1983, Fluid inclusion evidence for fluid mixing, Mascot-Jefferson city Zinc district, Tennessee: *Econ. Geol.*, v.78, p.1425-1439.
- Tempelman-Kluit, D., 1984, Meteoric water model for gold veins in a detached terrane: *GSA abstracts with programs*, v.16, p.674.
- Tempelman-Kluit, D., and D. Parkinson, 1986, Extension across the Eocene Okanagan crustal shear in southern British Columbia: *Geology* v.14, p.318-321.

Vikre, P.G., 1985, Precious metal vein systems in the National District, Humboldt County, Nevada: Econ. Geol., v.80, p.360-393.

Weir, R.H. Jr, and D.M. Kerrick, 1984, Mineralogical and stable isotopic relationships in gold-quartz veins in the southern Mother Lode, California: GSA abstracts with programs, v.16, p.688.

Wenner, D.B., and H.P. Taylor Jr., 1971, Temperatures of serpentinization of ultramafic rocks based on $^{18}\text{O}/^{16}\text{O}$ fractionation between coexisting serpentine and magnetite: Contrib. Mineral. Petrol., v.32, p.165-185.

White, G.P.E., 1984, South central district, B.C., in: B.C. Mineral Exploration Review, Infor. Circul, 1985b, p.36-38.

White, W.H., J.E. Harakel, and N.C. Carter, 1968, Potassium-Argon ages of some ore deposits in British Columbia: Can. Min. Metall. Bull., v.61, p.1326-1334.

XU, Guofeng, 1982, Mineragraphy, 188p. (in Chinese)

APPENDIX: SAMPLE LOCATIONS

1. Fairview deposit

F-7-F-9: quartz-schist, from near the entrance of the adit.

F-10-F-12: quartz, from a quartz vein about 50m northeast of the adit.

F-20-F-22: quartz, from a quartz vein about 150m southeast of the adit.

F-32: quartz, from a quartz vein about 300m northwest of the adit.

Others: see map "Fairview 3400F plan and sample locations".

2. Morning Star deposit

MP-1-MP-12: quartz, from waste dump.

Others: see map "Sampling locations of Morning Star deposit".

3. Stenwinder deposit

S-1-S-5: quartz, from a quartz vein about 100m northwest of the shaft.

S-6-S-7: quartz-schist, same location as S-1-S-5.

S-8-S-13: quartz and quartz-schist, from near the shaft.

SP-1-SP-6: quartz, from waste dump.

4. Oro Fino deposit

O-1-O-3: quartz, from near the shaft.

O-4-O-7: amphibolite, from near the shaft.

O-8-O-9: quartz, from the entrance of the shaft.

O-10-O-18: quartz, amphibolite and gneiss, from waste dump.

5. Twin Lake deposit

T-1: gneissic amphibolite, from about 300m north of the shaft.

T-2: schistified gneiss, from about 100m west of the shaft.

T-3-T-10: quartz, amphibolite and gneiss, from waste dump.

T-11-T-12: quartz, from quartz veins about 50m east of the shaft.

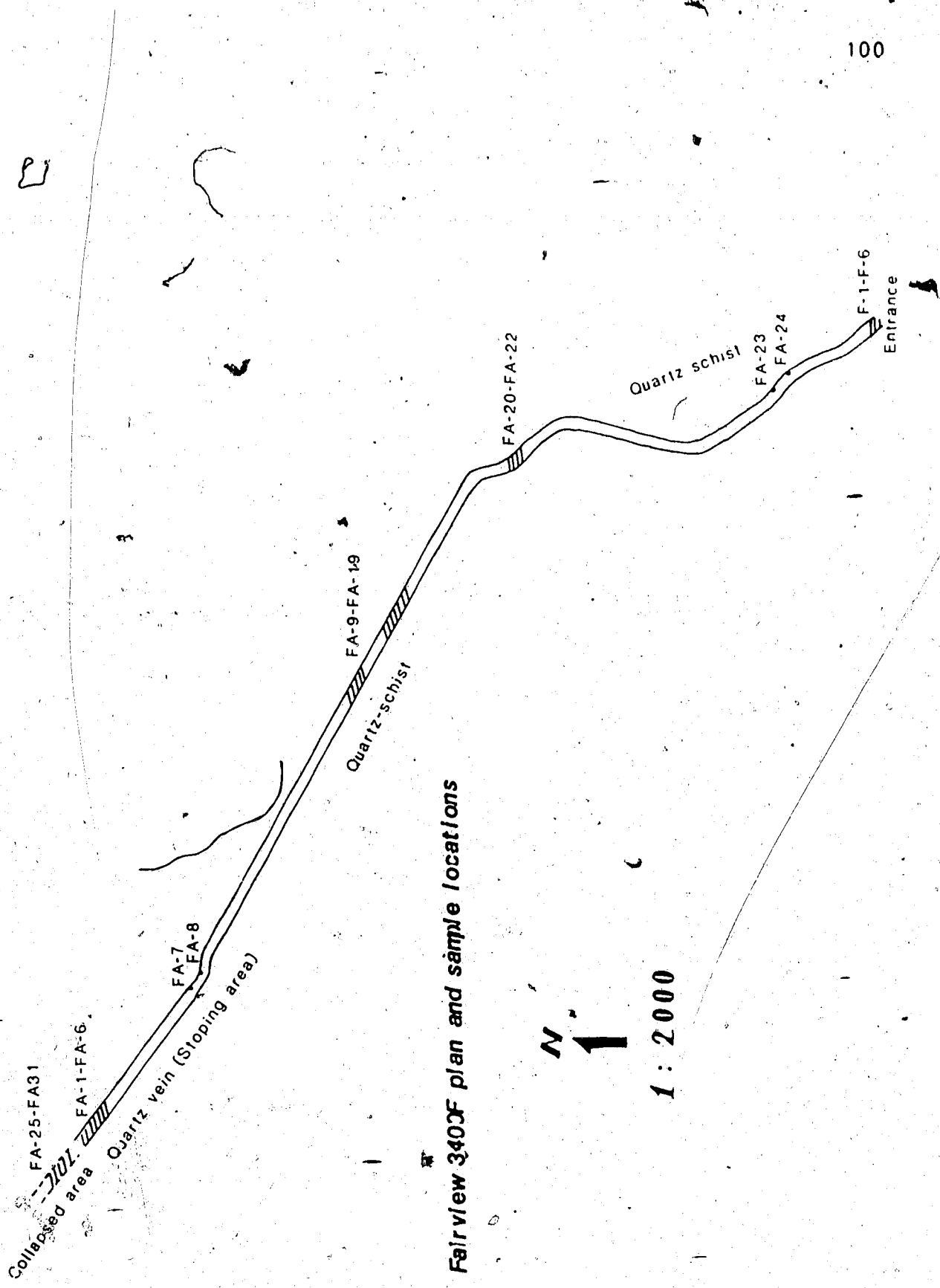
6. Dusty Mac deposit

D-3-D-18 and D-28-D-29: quartz and host rocks, within open pit.

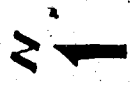
D-19-D-24: quartz, from about 1km northwest of the open pit.

DA-1-DA-9: country rocks, from 300-800m east of the open pit.

DB-10-DB-24: country rocks, from 200-800m west of the open pit.

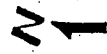


Fairview 340CF plan and sample locations



1 : 2000

Sampling locations of Morning Star deposit



1:2000

